Biomaterials Translational

Advances in electrode interface materials and modification technologies for brain-computer interfaces

Yunke Jiao[1], Miao Lei[1], Jianwei Zhu[1], Ronghang Chang[1], Xue Qu[1,2,3,]*

Key Words:
biomaterials; brain-computer interface; conductive polymer; interface materials; microstructure; neuroelectrode

From the Contents

ABSTRACT

Recent advances in neuroelectrode interface materials and modification technologies are reviewed. Brain-computer interface is the new method of human-computer interaction, which not only can realise the exchange of information between the human brain and external devices, but also provides a brand-new means for the diagnosis and treatment of brain-related diseases. The neural electrode interface part of brain-computer interface is an important area for electrical, optical and chemical signal transmission between brain tissue system and external electronic devices, which determines the performance of brain-computer interface. In order to solve the problems of insufficient flexibility, insufficient signal recognition ability and insufficient biocompatibility of traditional rigid electrodes, researchers have carried out extensive studies on the neuroelectrode interface in terms of materials and modification techniques. This paper introduces the biological reactions that occur in neuroelectrodes after implantation into brain tissue and the decisive role of the electrode interface for electrode function. Following this, the latest research progress on neuroelectrode materials and interface materials is reviewed from the aspects of neuroelectrode materials and modification technologies, firstly taking materials as a clue, and then focusing on the preparation process of neuroelectrode coatings and the design scheme of functionalised structures.

***Corresponding author:**
Xue Qu,
quxue@ecust.edu.cn.

http://doi.org/10.12336/biomatertransl.2023.04.003

How to cite this article:
Jiao, Y.; Lei, M.; Zhu, J.; Chang, R.; Qu, X. Advances in electrode interface materials and modification technologies for brain-computer interfaces. *Biomater Transl.* **2023**, *4*(4), 213-233.

Introduction

Since the discovery of electrical signals in the brain in the 1920s, people have been constantly searching for ways to decipher its thinking process and explore new methods of interaction between the human brain and the outside world. Brain-computer interface (BCI) recognises multiple electrical signals generated by the human brain during thought processes through neural electrodes, and converts them into meaningful information. This innovative approach does not rely on conventional extracerebral peripheral nerve-to-muscle output pathways but instead establishes a novel non-muscular channel between the human brain and computers or other electronic devices, enabling barrier-free interaction and control of information. The new non-muscular channel established between the human brain and computers or other electronic devices achieves barrier-free interaction and control of information. Implantable electrodes used to detect local neural signals have probes that can be embedded in designated areas of the cerebral cortex, providing a very high degree of accuracy in electroencephalogram signal transmission, while implantable BCIs can not only output and interpret human brain signals from the inside out, but also input and transform electrical signals from the outside in to reverse stimulate neurons and restore specific neural activity. BCI has provided a brand-new window for the study of brain activities and diagnosis of brain-related diseases,[1, 2] as well as serving as a novel treatment tool for neurological damage caused by diseases or injuries. For example, technological and theoretical advances in

neuroscience and implantable BCIs have introduced potential solutions for a wide range of common neurological-related disorders, including deafness, blindness, epilepsy, and depression.[3] Neuroelectrodes play a crucial role in signalling within BCIs as they determine the quality and efficiency of communication. This is essential to ensure the stable and effective operation of the BCI system. The electrode interface serves as the area where electrical, optical, and chemical signals are transmitted between the brain tissue system and external electronic devices. As the "bridge" of the BCI, it is also where the electrode material directly contacts biological tissues. The signal interaction ability, biocompatibility, and long-term stability of this interface directly impact the working efficiency and lifespan of BCI electrodes.

Currently, the mainstream neuroelectrodes on the market are still dominated by conventional electronic materials, such as metals and inorganic semiconductor materials; however, the high modulus of elasticity of the conventional electrode materials obviously leads to their inability to match the brain tissue. To solve this problem, electrode interface materials have been extensively investigated. One approach is to modify the structure of conventional metal and semiconductor electrode materials to enhance their flexibility. For example, a promising direction is to fabricate electrodes with smaller dimensions, such as thin films or filament structures.[4-6] Meanwhile, modifying the electrode surface with nanostructures,[7-9] such as modifying metal nanopatterns, or rough surface electrodes with nanoparticles, not only increases the surface area of the electrode interface and improves the contact with the neural tissue, but the surfaces with some specific structures also make the electrode interface have more biocompatible, which is more conducive to the neuron cell growth in the contact. After metals and semiconductors, another category that has received attention is the carbon nanomaterials for electrodes, which range from carbon quantum dots, carbon nanowires, and carbon nanotubes (CNTs), to graphene, and have variable structural features and therefore a wide range of tunable properties.[10-12] In addition, carbon nanomaterials have better biocompatibility than metals and semiconductor materials, as well as good electrical properties.[12-15] With the rise of conductive polymers (CPs),[16-18] more flexible organic materials have successfully expanded the choice of interface materials for neuroelectrodes. Polymer hydrogels as well as bio-based materials,[19, 20] as implants, possess better biocompatibility and even bioactivity, and have been widely used in the field of tissue repair and other areas since early days, and after improving the electrical properties through specific structures or doping with conductive components,[21-23] these organic materials have also demonstrated promising prospects in the field of neuroelectrodes.

In this review, we first introduce the biological responses of neuroelectrodes after implantation into brain tissues and the decisive role of the interfaces for electrode function. Afterwards, we review the latest research progress of neuroelectrode materials and interface materials from the aspects of neuroelectrode materials and modification technologies. Specifically, we discuss the materials used for neuroelectrodes as a starting point and subsequently delve into the preparation process of neuroelectrode coatings and the design of functional structures.

Challenges of Implantable Neuroelectrodes in Brain Tissue

Specificity of brain tissue

Brain tissue is one of the softest and most fragile tissues compared to other tissues in the human body.[24] Neural axons in brain tissue break at about 18% strain,[25] so rigid implants will inevitably cause damage to neural tissue when entering the brain. The brain and other central nervous tissues are mechanically protected throughout the body by other sturdy tissues, such as the dura mater and skull. Therefore, compared to other tissues, brain tissue is hardly exposed to mechanical stress from the outside nor does it generate as much internal mechanical stress as tissues such as muscles or blood vessels.[26] So once exposed to external mechanical stress, brain tissue is more susceptible to mechanical injury. Moreover, although brain tissue has a regenerative mechanism, self-repair of neural tissue after damage is difficult. One point is due to the unfavourable microenvironment formed by post-injury inflammation, and the second is the lack of healthy extracellular matrix, and the presence of neuroglial scarring affects neuronal survival, regeneration and axonal growth.[27]

Foreign body reaction after electrode implantation

Foreign body reaction inevitably occurs when implanting any material into the tissues of a living organism,[28] and similarly, foreign body reaction occurs during the implantation of neuroelectrodes into brain tissues. The first and most critical event that occurs during the implantation of electrodes is the disruption of the blood-brain barrier,[29, 30] where the infiltration of blood cells and plasma proteins triggers a series of dynamic biochemical alterations and an inflammatory cascade with multicellular involvement at the tissue-electrode material interface. Within minutes after blood-brain barrier injury, resting microglia are activated as primary effectors, transforming into a "pro-inflammatory" phenotype[31] and initiating an acute immune response. In the following hours, oligodendrocytes are activated and begin to participate in neuronal repair.[32] And in the subsequent days, astrocytes are activated by interleukin-1β, tumour necrosis factor-α, and complement component 1q from microglia,[33] and gradually accumulate near the electrode and form a glial scar.[34] Further, activated astrocytes no longer provide an appropriate nerve regeneration matrix while synthesising and secreting inhibitory and damaging factors leading to neuronal loss and reduced fibre density.[35] In summary, the stress response initiated by

1 Key Laboratory for Ultrafine Materials of Ministry of Education, School of Material Science and Engineering, Frontiers Science Center for Materiobiology and Dynamic Chemistry, East China University of Science and Technology, Shanghai, China; 2 Wenzhou Institute of Shanghai University, Wenzhou, Zhejiang Province, China; 3 Shanghai Frontier Science Center of Optogenetic Techniques for Cell Metabolism, Shanghai, China

microglia undergoes several days of indirect cellular forces that ultimately prevents the intimate contact and communication between neurons and electrodes, both in terms of physical space and biochemical cues. And when the electrodes are implanted in brain tissue, a highly dynamic and complex inflammatory microenvironment consisting of multiple cells and factors forms on their surface, thereby impeding direct dialogue between neurons and the electrode surface.

Literature Search

Articles on neuroelectrode materials for BCIs and neuroelectrode coating technology were searched using the search terms: "brain-computer interfaces" or "neuroelectrodes" combined with "coating materials", "coating technology", and "microstructure", respectively. These searches were conducted on the Web of Science in July 2023, and articles published after 2018 have been collected in order of publication. After careful screening, 145 articles were included in this review.

Interface Determines Electrode Function

Electrical properties

The most basic function of implantable microelectrodes is to acquire electrophysiological signals from neurons, and the signal quality is reflected in several metrics, including signal-to-noise ratio, single-unit recording capability, and long-term recording capability.[36, 37] In BCI systems, ions are the carriers of signals transmitted along the nerve, and electrons are the medium in the electrode. Therefore, the neuroelectrode interface is where the ionic signals are converted into electronic signals, and the electrical properties of the neuroelectrode, such as the interface impedance between the electrode and the brain tissue, and the amount of charge storage, determine the quality of the signals recorded by the electrode.[38, 39] The interfacial impedance, in turn, is affected by the roughness of the neuroelectrode interface, its area, and the electrical/ion exchange capacity of the interfacial material.[40]

Biocompatibility

Biocompatibility is reflected in several aspects. Firstly, the electrode material itself should be non-biotoxic. Secondly, it should cause as little mechanical damage to the brain tissue as possible during and after implantation, and lastly, it should induce as little immune response as possible during long-term use. Mechanical damage caused during the implantation of neuroelectrodes is the beginning of the immune response, which triggers a series of inflammatory cascade reactions that will firstly disturb the local tissue microenvironment around the neuroelectrode, thus affecting the collection of electrophysiological signals from the electrode to the surrounding area.[41-43] In contrast, reducing the size of the implant[44-46] and increasing its flexibility[47-49] are methods to minimise mechanical damage to the implant. The long-term biocompatibility of the electrodes after implantation, on the other hand, is challenged by the ability to adapt the elastic modulus of the neuroelectrode to the brain tissue,[50-52] the ability of the electrode interface to inhibit immune responses,[53-55] and the stability of the electrodes during long-term use.[56-58]

Bioactivity

Bioactivity is a higher requirement for current neuroelectrode interfaces. Biocompatibility aims to make the implant "invisible" to biological tissues, thus escaping immune tracking and minimising the impact of immune responses. However, due to the unavoidable damage caused by implantation and the difficulty of repairing neuronal cells that are damaged, biocompatibility alone cannot meet the requirement for high quality signal transmission. To achieve the goal of non-destructive implantation, the neuroelectrode needs to be bioactive. In other words, through specific morphology of the electrode interface[59, 60] and modification of the bioactive components,[61-63] the neuronal cell repair can be actively regulated, and the neural axon growth can be promoted, so that the neural tissues around the electrodes can restore the pre-implantation state, and even establish a tighter connection.

Neuroelectrode Materials

Inorganic materials

Metal and inorganic semiconductor materials are traditional neuroelectrode materials with good chemical inertness and electrical properties, but it is often difficult for metal and semiconductor materials to adapt to the needs of brain tissues for elastic modulus and biocompatibility. In recent years, researchers have made progress in improving the performance of neuroelectrodes made of inorganic materials by designing the composition and structure of neuroelectrodes made of metals and semiconductors. Meanwhile, the rise of new carbon nanomaterials, such as nanodiamond, CNTs, and graphene, has also provided new directions for inorganic neuroelectrodes. Carbon nanomaterials have great potential in the field of neuroelectrodes due to their extremely low toxicity, high biocompatibility and unique optical, electrical, magnetic and chemical properties.

Metal electrodes

Traditional metal electrodes often use precious metals such as aurum (Au), platinum (Pt), etc. Precious metals have good electrical conductivity and chemical stability, but their excessive elastic modulus makes them difficult to be compatible with brain tissue. One way to reduce the elastic modulus of metal electrodes is to make the metal partially ultrathin.[64-66] For example, cylindrical three dimensional (3D) Au thin-film microelectrodes fabricated using the microelectrode array (MEA) technique, with the sidewalls insulated with poly(parylene C) and the tip modified by wet etching and/or the application of a titanium nitride coating, exhibit low impedance and low intrinsic noise levels.[4] Hong et al.[67] developed nucleation-inducing seed layers using biocompatible polyelectrolyte multilayer metal films using flexible and transparent ultrathin (< 10 nm) Au MEAs (**Figure 1A**) with low sheet resistance (< 5 Ω^{-1}), high light transmission (> 77%), and excellent mechanical bending performance (600 mm bending radius for one cycle) (**Figure 1B**). Miniaturising metal electrodes is an effective way to increase their flexibility, but the size of bioelectrode materials is limited by the electron mean free range, and materials with sizes smaller than the electron average free range inhibit electron mobility. Lim et

al.[68] prepared a nanocomposite of whiskered Au nanosheets (**Figure 1C**). While possessing high tensile properties, the permeation threshold (1.56 vol%) was maintained below that of Au nanoparticles (5.02 vol%) and Au nanosheets (2.74 vol%).

Another category of metallic materials suitable for neuroelectrodes is room-temperature liquid metals (LMs) such as gallium-based alloys that are liquid at room temperature. LMs show potential for neuroelectrodes due to their fluidity, high electrical conductivity, and high biocompatibility.[69-71] LM-based fluidic cuff electrodes, which are highly flexible and maintain excellent electrical conductivity even when stretched to 200% of their original length, are capable of transducing peripheral nerve signals and delivering neural stimuli for up to 2 weeks under exercise.[72] Zhang et al.[71] developed a 20-channel neuroelectrode array based on the eutectic Ga–In alloy (75.5% gallium and 24.5% indium) in a 20-channel neural electrode array. Electrochemical impedance spectroscopy tests showed that the studied LM electrode has a similar interfacial impedance to the Pt electrode; the maximum and minimum impedances of the LM-type electrode are 0.75 MΩ/4.1 kΩ (2.77 MΩ/5.2 kΩ for the Pt electrode), in the same range, over the test frequency range of 1×10^{-1}–1×10^{5} Hz (**Figure 1D**). Dong et al.[69] prepared highly stretchable neural electrode arrays by screen-printing an LM conductor onto a poly(dimethylsiloxane) substrate (**Figure 1E**), which exhibited stable electrical properties at 100% strain. However, the chemical properties of LMs under physiological conditions limit their *in vivo* application, e.g., in environments above 1 ppm oxygen content, an oxidised layer rapidly forms on the surface of Ga, leading to a decrease in conductivity at the interface.[73, 74]

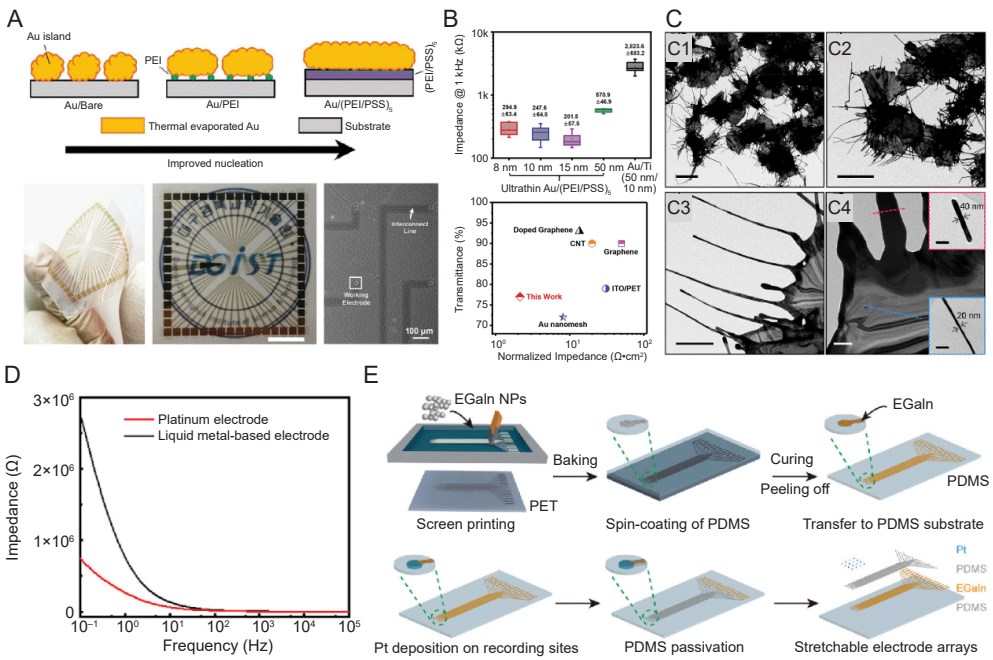

Figure 1. New metal material electrode. (A) Schematic of the formation process of ultrathin Au electrodes on polyelectrolyte coatings and photographic and microscopic images of Au/$(PEI/PSS)_5$ MEA on plastic. (B) The magnitude of the impedance at 1 kHz (top) and a comparison of the area-normalised electrochemical impedance and light transmittance in a recently developed neuro-microelectrode (bottom). A and B were reprinted from Hong et al.[67] Copyright 2022 Wiley-VCH GmbH. Reproduced with permission. (C) TEM images of whiskered Au nanosheets showing the overall morphology and magnified views of the edge portion of the whiskers. Scale bars: 5 μm (C1, C2), 1 μm (C3), 200 nm (C4). Reprinted with permission from Lim et al.[68] Copyright 2022 American Chemical Society. (D) The EIS curves of the LM-based and Pt electrodes under 1×10^{-1} up to 1×10^{5} Hz at a scan rate of 0.1 V/s (in normal saline, 10 mV sine wave).[71] (E) Fabrication of stretchable metal electrodes based on liquid metal-polymer conductors using screen printing, which reprinted from Dong et al.[69] Copyright 2021 Wiley-VCH GmbH. Reproduced with permission. Au: aurum; EGaIn: eutectic gallium–indium alloy; EIS: electrochemical impedance spectroscopy; LM: liquid metal; MEA: microelectrode array; NP: nanoparticle; PDMS: poly(dimethylsiloxane); PEI: polyethylenimine; PET: polyethylene terephthalate; PSS: poly(styrene sulfonate); Pt: platinum; TEM: transmission electron microscopy.

Semiconductor materials

Semiconductor materials are rich in composition and structure, and can be tuned and processed to exhibit a variety of properties and produce a multitude of functions to suit applications in different scenarios.

Traditional silicon-based electrodes can conform to brain movements when processed into microneedle arrays on flexible stretchable substrates. Lee et al.[75] demonstrated a 1024-channel penetrating silicon microneedle array using a double-sided lithographic microfabrication process (**Figure**

2A–C) to successfully record single-cell activity in mice under both optogenetic and whisker-air blowing stimuli for up to 196 days. Suzuki et al.[76] used a complementary metal oxide semiconductor MEA with 236,880 electrodes each measuring 11.22 μm^2 and covering an area of 5.5 × 5.9 mm^2 to provide a detailed single-cell level neural activity analysis platform for brain slices, human induced pluripotent stem cell-derived cortical networks, peripheral neurons, and organ tissues of the human brain. Two-dimensional transition metal carbides (MXene) have excellent metal conductivity, electrochemical stability, and higher volumetric capacitance than conventional carbon-based electrode materials.[77-79] Rafieerad et al.[78] prepared a novel Ta4C3Tx MXene-tantalum oxide hybrid-structure electrode based on MXenes, innovatively using a fluorine-free etching technique to achieve superior bulk capacitance while maintaining biocompatibility. As shown in **Figure 2D**, the titanium dioxide (TiO_2)-based electrode arrays of reconfigurable anatase-brookite bicrystalline polycrystalline mesoporous layers exhibited excellent selectivity and fast photoconductive response to ultraviolet radiation, high stability in aqueous solution while maintaining a high switching ratio of 10 for 5 more than 30 days, and excellent biocompatibility for cell transfer and growth.[80] Zhang et al.[81] developed an active fully transparent electrocorticography array based on zinc oxide thin-film transistors (**Figure 2E**, and **F**) with a transparency of up to 85% and a higher signal-to-noise ratio than Au grid electrodes (zinc oxide thin-film transistors 13.2 dB, Au grids 19.9 dB).

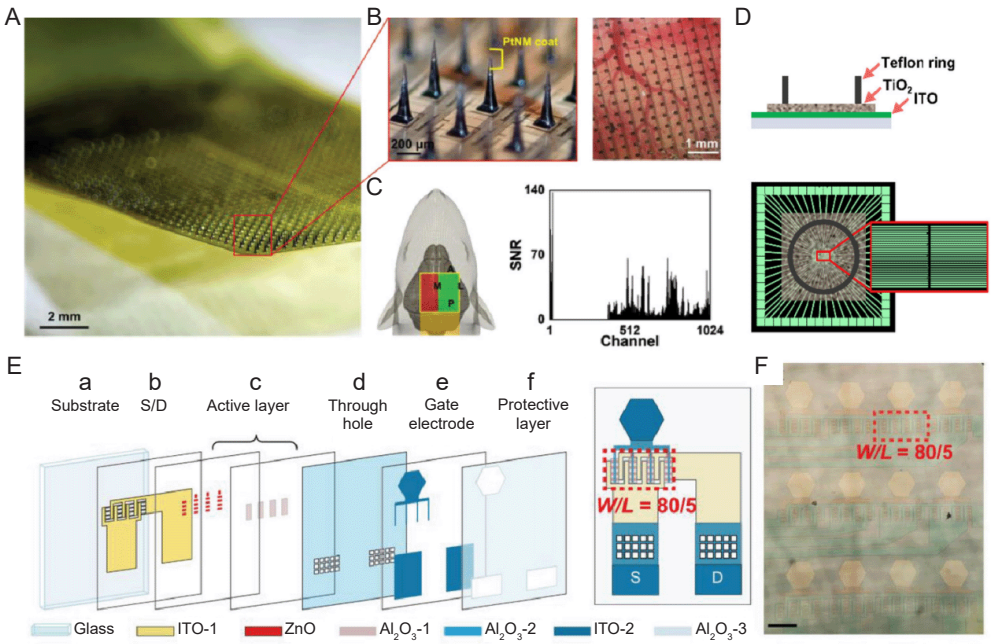

Figure 2. Semiconductor materials neuroelectrodes. (A) Photograph of a 1024-channel SiMNA and a magnified view of an array with a tapered SiMN with a height of approximately 300 μm and a tip coated with PtNM. Scale bar: 2 mm. (B) Magnified view of a 1024-channel SiMNA implanted in the right hemisphere of the rat brain. Scale bar: 200 μm (left), 1 mm (right). (C) Schematic diagram of SiMNA implantation in the right hemisphere with electrical connections pointing toward the back of the rat (green highlighted area indicates successful implantation of cortical SiMNs, while the SiMN in the red highlighted area is located at the top of the rat skull) and a signal-to-noise histogram of whisker blowing stimulation evoked LFP response. A–C were reprinted from Lee et al.[75] Copyright 2022 Wiley-VCH GmbH. Reproduced with permission. (D) Side and top views of patterned TiO_2 electrodes. The green parallel lines in the top view represent ITO patterns attached to 60 external contact pads.[78] (E) Left: (a, b) The first ITO layer of 100-nm thickness for source and drain, (c) 20-nm thick ZnO active layer and the first Al_2O_3 layer of 10-nm thickness for the ZnO layer protection, (d) the second Al_2O_3 layer of 20-nm thickness as the gate dielectric layer and through-holes punched in the layer, (e) the second ITO layer of 100-nm thickness for the gate electrodes, and (f) the third Al_2O_3 layer of 20-nm thickness to protect the whole device. Right: Structure of a ZnO-TFT electrode. The red dashed square labels a transistor with W/L = 80/5, which consist of 16 transistors with W/L = 5/5 in parallel. (F) Microscopic image of a 3 × 4 ZnO-TFT array. The red dashed frame labels an active region consisting of 16 paralleled ZnO-TFT, corresponding to that in the red dashed frame in E (right). Scale bar: 200 μm. E and F were reprinted from Zhang et al.[81] Al_2O_3: aluminum oxide; D: drain; ITO: indium-tin-oxide; LFP: local field potential; PtNM: platinum nanomesh; S: source; SiMNA: silicon microneedle array; SNR: signal-to-noise ratio; TFT: thin-film transistor; TiO_2: titanium dioxide; W/L: width-to-length ratio; ZnO: zinc oxide.

Carbon nanomaterials

Carbon nanomaterials, ranging from carbon quantum dots, CNTs to graphene, have versatile structural features, which also contribute to the special functionality of carbon nanomaterials, which are widely used as neuroelectrode materials on the basis of possessing high chemical stability and biocompatibility.[82-84] Flexible CNT fibre were able to continuously record signals from the spinal cord of freely moving rats for 3–4 months

without electrode repositioning and successfully recorded individual neurons and local field potential activities in response to mechanical stimulation of somatic cells.[85] Yang et al.[86] developed a flexible multifunctional electrode based on CNT arrays, which, compared with conventional Au electrodes, has a larger electrochemically active area (3.54 times), higher specific capacitance (13.75 times) and charge storage capacity (2.66 times). As shown in **Figure 3A**, Xiong et al.[87,88] prepared a multilayer graphene hydrogel membrane by flow self-assembly of chemically transformed graphene nanosheets. Although Young's modulus of this multilayer graphene hydrogel membrane was not sufficient to match the nerve tissue, there was almost no inflammatory response after 8 weeks of implantation in the sciatic nerve of rats. It can be concluded that due to the sliding between the graphene mizunas, the multilayer graphene hydrogel membrane showed significant viscoelasticity, which enhanced contact while reducing compression (**Figure 3B**), thus reducing inflammation due to the stiffness mismatch. Xiong et al.[89] developed a graphene-based fibre optical electrode, which dramatically enhanced the charge storage capacity of the graphene fibre electrode while maintaining the excellent electrical properties of the graphene fibre electrode, which was able to safely deliver stimulation currents up to 504.04 mC/cm^2.

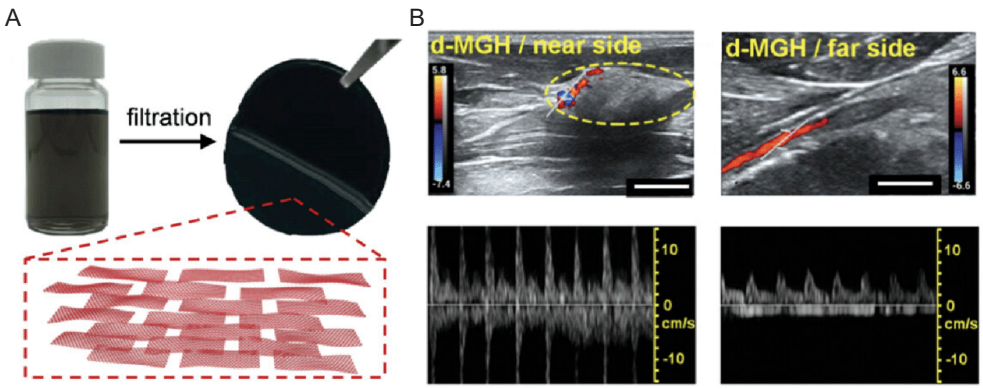

Figure 3. Neuroelectrodes are made of carbon nanomaterials. (A) Photograph of graphene dispersion and MGH membrane (top). The inset (bottom) outlines the multilayer structure of the MGH membrane made of CCG nanosheets (red).[87] (B) Proximal and distal d-MGH at 8 weeks after implantation. The color bars represent the blood flow velocity. Scale bars: 5.0 mm (left), 2.0 mm (right).[87] CCG: chemically converted graphene; d-MGH: CCG nanosheets densely packed MGH; MGH: multilayer graphene hydrogel.

Conductive polymers

CP materials provide a softer interface and excellent biocompatibility while being able to guarantee the required electrical properties of nerve electrodes.[90-92] Hydrogels have a tunable 3D structure, are water-rich and have a low modulus of elasticity, as can imitate the chemical-mechanical properties of neural tissues, and CP hydrogels are therefore widely used as neuroelectrode materials. Liang et al.[93] used polypyrrole (PPy)-modified microgel as a cross-linking agent to generate electrically conductive transparent hydrogels. By restricting the conductive components to the surface of the microgel, the interaction between the particles and light waves was reduced, thus improving the transparency of the hydrogel while maintaining good electrical conductivity. Xia et al.[94] developed a set of polymer network hydrogels interpenetrated with poly(N-isopropylacrylamide) and poly(Cu-arylacetyl) (HCuM). Poly(Cu-arylacetates) has intrinsic electronic conductivity and unique fluorescent properties for optoelectronic, photocatalytic, and bioimaging applications. The presence of the poly(Cu-arylacetylide) component allows it to exhibit extreme adhesion, resistance to swelling (**Figure 4A**, and **B**), excellent antimicrobial properties, and high biocompatibility. Hydrogels have a wide range of advantages as neuroelectrode materials, but the inherent electrical conductivity is generally poor and other methods are needed to enhance their electrical properties. Among these, doping of nanometallic materials (nanowires, nanosheets or nanoparticles) and carbon materials (nanotubes or graphene) are common ways to improve the conductivity of hydrogels. Rinoldi et al.[95] developed a flexible neuroelectrode interface material consisting of a polyacrylamide hydrogel loaded with plasmonic Ag nanocubes. The incorporation of Ag nanocubes enabled the hydrogel to obtain excellent conductive properties, with a 2.4-fold enhancement in conductivity at 10 Hz compared to pure polyacrylamide hydrogel (**Figure 4C**, and **D**). Won et al.[96] prepared conductive fibres doped with Au nanoparticles in the outer layer by using osmotic pressure to control the distribution of Au ions in the polymer network, and the uptake and reduction of the Au precursor in polyurethane fibres. High electrical conductivity ($\sigma = 7.68 \times 10^4$ S/m) and low impedance ($|Z| = 2.88 \times 10^3\ \Omega$) were obtained while maintaining the original modulus of elasticity of the polyurethane fibres.

Poly(3,4-ethylenedioxythiophene):poly(styrene sulfonate) (PEDOT:PSS) hydrogels[97-99] have attracted much attention among CP hydrogels due to their higher electrical conductivity induced by well-connected CP networks.[100-102] Li et al.[103] designed a stretchable network electrode by combining the CP PEDOT:PSS hydrogel as a top layer with a resilient polystyrene-ethylene-butylene-styrene substrate bond. It is characterised by the use of a network design with a large strain range, which maintains a remarkably high level of electrical properties under huge strains compared to conventional electrodes.

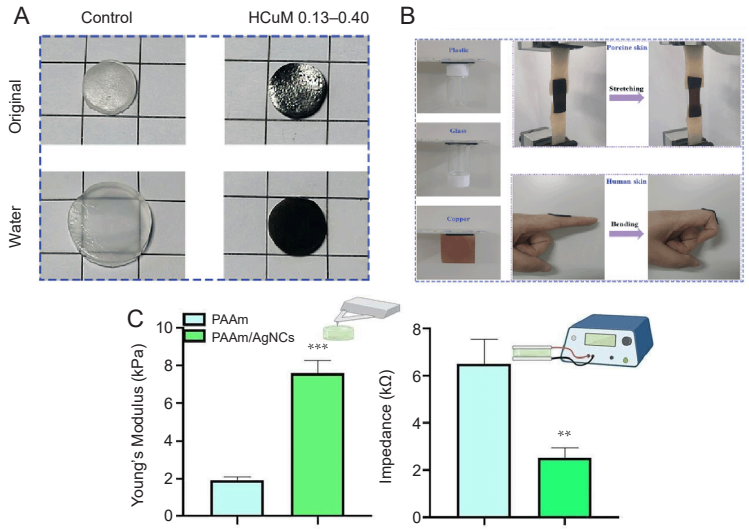

Figure 4. Neuroelectrodes are made of conductive polymer materials. (A) Swelling study of pNIPAm hydrogel and HCuM 0.13–0.40 in water for 5 days. (B) Demonstration of adhesion of HCuM 0.13–0.40. A and B were reprinted from Hong et al.[94] Copyright 2022 Wiley-VCH GmbH. Reproduced with permission. (C) Histogram of Young's modulus, showing the mechanical properties of PAAm/AgNCs compared to PAAm hydrogels, measured by nanoindentation method (left) and histogram of the electrical impedance values , measured at a physiologically significant frequency (10 Hz), showing the superior electrical properties of the PAAm/AgNCs hydrogel (right). Data are expressed as mean ± SD. $^{**}P \leq 0.01$, $^{**}P \leq 0.001$. Reprinted with permission from Rinoldi et al.[95] Copyright 2023 American Chemical Society. AgNC: silver nanocube; HCuM: a set of polymer network hydrogels interpenetrated with poly(N-isopropylacrylamide) and poly(Cu-arylacetyl); PAAm: polyacrylamide.

Bio-based materials

Biobased materials are characterised by high biocompatibility, biodegradability, and sustainability, whereas biopolymers such as hyaluronic acid,[104] alginate,[105, 106] chitosan,[107, 108] filipin,[109-111] and collagen[112-114] not only possess the general characteristics of biobased materials, but also low immunogenicity, anti-inflammatory, and even bioactivity.[115] These biological properties, which are difficult to be possessed by inorganic and polymer materials, have led to the widespread interest in bio-based materials in the field of neuroelectrodes. Zhou et al.[116] designed a hybrid probe consisting of multiple flexible MEAs wrapped in silk proteins. Zhou's team took advantage of the properties of silk proteins, which have a high stiffness when dry and a significant decrease in stiffness after absorbing water, to design a neuroelectrode that actively adapts to its environment. The filipin-coated probes remain hard before implantation to facilitate surgical implantation, and after implantation, the filipin softens when it comes into contact with body fluids and absorbs water, which reduces its mechanical strength and allows it to remain mechanically compliant with the surrounding tissue. This variable mechanical property ensured high-fidelity implantation of the electrodes, and the electrode worked appropriately and elicited a small immune response when observed 2 months after implantation. Yang et al.[117] used bacterial cellulose, a flexible substrate synthesised by microorganisms with low mechanical strength, as the electrode substrate material to fabricate a bacterial cellulose-based neuroelectrode system, and eight weeks after implantation, the bacterial cellulose electrodes remained conformally adhered to the surface of the surrounding tissues and maintained the curvilinear shape with minimal immunoreactivity.

Neuroelectrode Interface Materials

In addition to designing the structure and performance of the electrode body material, decorating the basic electrode with functional coating materials is another feasible solution to the functional limitations of the electrode body. The electrode interface is the area where the electrode body is in direct contact with the brain tissue, and it is also an important area for the transmission of electrical signals and cellular activities. Therefore, it can be considered that the performance of this interface determines overall electrode functionality. As an interface material, coatings can exist temporarily or permanently alongside the body electrode, providing a functional surface that extends or compensates for its capabilities.

In terms of modulating the bioactivity of the implanted materials, some studies have doped anti-inflammatory agents,[118] cell attachment molecules,[119, 120] and neurotrophic factors[121, 122] into the coating materials to improve the microenvironment around the neuroelectrodes and coordinate the biological responses of different cell types through passive diffusion or controlled delivery. In addition, well-designed coatings can provide micro-woven surfaces, such as microconical structures or random nano-textures that match the cellular characteristics of neurons. These textured surfaces or 3D structures located at cellular and subcellular scales can modulate the immune response of glial cells, promote direct neuronal attachment and growth, as well as synaptic growth and extension, and strengthen neuronal survival.

Metal coating

Although traditional precious metal materials possess extremely high electrical conductivity, it is often difficult to avoid the problem of mismatch between elastic modulus and brain tissue when used for the electrode body, but using nano-metallic materials for the coating material of flexible electrode substrate is another approach to solve the problem.

Through adjusting the immersion and exudation time, a network of Au nanoparticles was formed on the polymer fibre shell, which showed excellent electrical properties (conductivity 7.68×10^4 S/m impedance 2.88×10^3 Ω at 1 kHz) with an elastic modulus approximating the brain tissue and achieved stable recording of electrical signals for up to 4 months.[96] In addition to being used to improve organic flexible electrode material substrates, metal coatings are often used to modify metal electrodes because the added coating does not affect the biocompatibility of the original electrode when the electrode substrate is identical to the coating material. Ramesh et al.[123-125] performed pulsed direct-current electrophoretic deposition of laser-generated platinum nanoparticles on platinum-based 3D neuroelectrodes and found that this coating of platinum nanoparticles was sufficiently stable (**Figure 5A**) and the total mass of platinum around the electrodes was below the systemic toxicity-related concentrations after 4 weeks of experiments in the rat brain. By functionalising the metal coating with a structural design, the liquid can improve the performance of the electrode without changing the coating material. The internal structure and surface morphology of metal electrodes also affect the flexibility, electrical conductivity, and biocompatibility of neuroelectrodes. As shown in **Figure 5B**, Yang et al.[126] proposed a dual-microcrack coupling strategy to enhance the stretchability of metal electrodes by utilising the complementarity between two layers of Au microcracked films. The double-microcrack-coupled electrode fabricated using this method has a much lower resistance change (R/R0 = 5.6) and exhibits a high stretchability of ~200% at 100% strain (**Figure 5C**, and **D**).

Inorganic coatings

The combination of inorganic semiconductor materials and metal electrode substrates can achieve controllable tuning of the electrical properties of neuroelectrodes. The impedance and intrinsic noise level of microelectrodes were successfully reduced by modifying titanium nitride coatings by wet etching on micro-Au cylindrical MEAs.[4] Nguyen et al.[127] designed a wide bandgap material system consisting of silicon carbide (SiC) nanomembranes as the Faraday interface and silicon dioxide (SiO_2) as the encapsulation layer, which, while maintaining the bio-interface and biosensing functions, showing remarkable electrical stability (**Figure 5E**). The hybrid structure of SiC/SiO_2 is extremely resistant to degradation and can guarantee the proper functioning of the underlying electronic components for at least a decade, with the potential for long-term sustained use over the lifetime of the patient. Cyclic bending test surfaces that the hybrid structure has excellent mechanical flexibility and electrical stability, and is able to form conformal contacts with biological tissues.

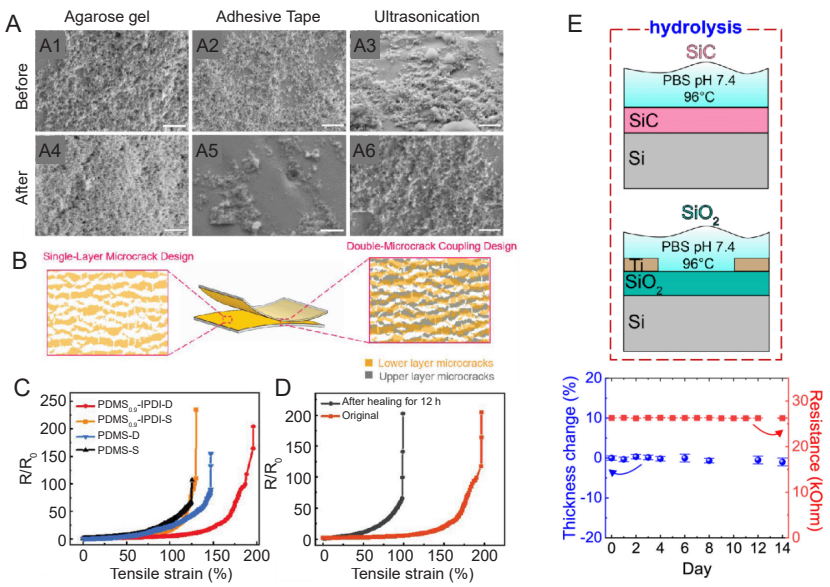

Figure 5. Coating of metallic materials for neural electrodes. (A) SEM images of the side of the PDC-coated neural electrode before (A1–3) and after (A4–6) mechanical stability tests. Scale bars: 500 nm.[123] (B) Schematic diagrams of stretchable electrodes based on a single-layer microcrack design and a dual microcrack-coupled design. (C) R/R0 *versus* tensile strain for Au electrodes based on PDMS 0.9-IPDI and PDMS substrates, respectively (-D for a double-layer microcrack, -S for a single-layer microcrack). (D) Dual microcrack-coupled PDMS 0.9-IPDI electrodes Change in tensile resistance after 12 hours of healing at 25°C. B–D were reprinted from Yang et al.[126] Copyright 2023 Wiley-VCH GmbH. Reproduced with permission. (E) Soaking test of hydrolysis in SiC and as-grown SiO_2 in 1× PBS at different temperatures up to 96°C (top) and SiC thickness and electrical resistance variations after the accelerated hydrolysis test in PBS at 96°C after up to 14 days (bottom).[127] Au: aurum; IPDI: isophorone diisocyanate; PBS: phosphate buffer solution; PDC: pulsed direct current; PDMS: poly(dimethylsiloxane); R/R0: resistance change; SEM: scanning electron microscope; SiC: silicon carbide; SiO_2: silicon dioxide; Ti: titanium.

Carbon materials are also frequently used as coating materials for neuroelectrodes due to their excellent electrical conductivity and good biocompatibility. Pt/iridium (Ir) neuroelectrodes coated with graphene oxide, fabricated using electrochemical reduction techniques, resulted in a 15.2-fold increase in charge storage capacity and a 90% reduction in impedance with only a 3.8% increase in electrode diameter.128 A hybrid coating of reduced graphene oxide and Pt was able to reduce impedance by a factor of 60 by electrodeposition on planar Pt microelectrodes, allowing long-term detection of neural spike potentials in epileptic mice.[129] Liu et al.[82] modified conventional metallic silver electrodes with graphene to form a van der Waals heterostructure at the interface. The graphene/silver electrode interface impedance was reduced to 161.4 ± 13.4 MΩ/μm^2, and the cathode charge storage capacity reached 24.2 ± 1.9 mC/cm^2, which was 6.3 and 48.4 times higher than that of commercial silver electrodes, respectively.

Conductive polymer coatings

CPs can be used both as a substrate material for neuroelectrodes and as a modified coating material for neuroelectrodes. The construction of hydrogel networks using CPs can confer other important characteristics required for their neuroelectrode materials, such as bioadhesion, flexibility, and antifouling ability. One study prepared a PEDOT/polydopamine melanin coating (**Figure 6A**) by doping polydopamine melanin with PEDOT, which enabled it to exhibit better electrochemical and mechanical stability than PEDOT/PSS and was able to maintain cell proliferation and even promote cell differentiation into neuronal networks (**Figure 6B**, and **C**).[130] Saunier et al.[131] electrochemically method by depositing carbon nanofibres with PEDOT on Au MEAs to prepare PEDOT:carbon nanofibre thin film coatings. The synergistic effect of carbon nanofibres and PEDOT resulted in coatings with remarkable electrochemical properties combining low impedance, high charge injection capability, and reliable neurotransmitter monitoring. The properties of CPs are affected by doping compositions and synthesis modes, and in addition to varying the CPs'. In addition to changing the doping composition of CPs, the use of different polymerisation techniques can also lead to tunable properties of CPs. Some studies have used chemical polymerisation to directly polymerise PEDOT on the electrode sites, obtaining similar impedance and good stability to that of electro-polymerisation, which greatly improves the modification efficiency of multichannel electrodes compared to electro-polymerisation.[132] Lim et al.[133] encapsulated Ga-based LM electrodes with PEDOT:PSS by electrochemical deposition to prevent LM from oxidising and degrading under physiological conditions. The study showed that the PEDOT-encapsulated LM electrodes, in a 6-week invertebrate model, recorded statistically higher signal-to-noise ratios compared to those of bare LM (P = 0.017) versus conventional platinum electrodes (P = 0.061; **Figure 6D**).

However, weak adhesion between PEDOT and metal electrodes is common, and unstable connections can easily lead to coating detachment thus leading to interface failure and loss of PEDOT functionality. There have been several previous attempts to improve the adhesion of PEDOT coatings, such as roughening the substrate material134 and introducing functional groups into the PEDOT monomer for modification.[135, 136] All of these approaches have made progress in enhancing the adhesion of PEDOT coatings, but there are still problems such as affecting the interfacial conductivity. Tian et al.[137] pre-polymerised thin layers of polydopamine (PDA) as an adhesive and then electropolymerised it with hydroxymethylated 3,4-ethylenedioxythiophene with PSS to form a stable interpenetrating PEDOT-MeOH:PSS/PDA network. The interfacial adhesion of the PEDOT-MeOH:PSS/PDA interface to the metal electrode substrate was significantly improved, retaining 93% of the area after 20 minutes of vigorous sonication, and the interfacial impedance was reduced by two orders of magnitude compared with that of the uncoated platinum-iron wire microelectrode.

Active substance grafting

A significant reason for the reduced signal reception efficiency of nerve electrodes during service is the contamination of nerve electrode materials with biomolecules from biological fluids, such as nonspecific adsorption of proteins such as bovine serum albumin, lysozyme and fibrinogen. Modification of antifouling molecules on the surface of neuroelectrodes can effectively reduce biomolecule adsorption, attenuate inflammatory responses and prolong the service life of neuroelectrodes. Lubricin is a biological anti-adhesion glycoprotein that rapidly self-assembles and firmly adheres to most interfaces including PPy (**Figure 7A**), resulting in an easy-to-apply and efficient coating.[138] Amphiphilic ion coatings are another common class of antifouling coatings, such as carboxybetaine, sulfobetaine, and phosphatidylcholine, which are active substances that enhance the hydrophilic properties of neuroelectrode surfaces. An ultrathin sulfobetaine coating consisting of PDA, polyethyleneimine, and poly(sulfobetaine methacrylate-co-methacrylic acid), was able to completely inhibit fibroblast adhesion *in vitro*, preventing cell adhesion for at least 31 days and maintaining stable electrode impedance.[139] Another study used a methacryloyloxyethyl phosphorylcholine coating polymerised *in situ* by gamma radiation to introduce antifouling properties to the surface of PPy, which showed excellent resistance to biofouling without affecting the conductivity of the electrode body and reduced scar tissue formation *in vivo*.[140] Lee et al.[141] designed a virtually frictionless lubrication layer modification with a silicon-based neural probe, where the surface of the probe was functionalised with hydroxyl (-OH) groups by oxygen (O_2) plasma treatment, and then a self-assembled monolayer was formed with trichloro(1H,1H,2H,2H-perfluorooctyl)-silane using gas-phase deposition. As shown in **Figure 7B**, the lubricant layer-modified probe implantation friction was reduced by 86-fold, and the expression levels of ionised calcium-binding adapter molecule 1 and glial fibrillary acidic protein were significantly reduced in microglia and astrocytes in the vicinity of the probe.

Composite coating

As the "bridge" between brain tissue and external equipment, the interface of neuroelectrode needs to coordinate the dual needs of biological tissue and mechanical equipment, although

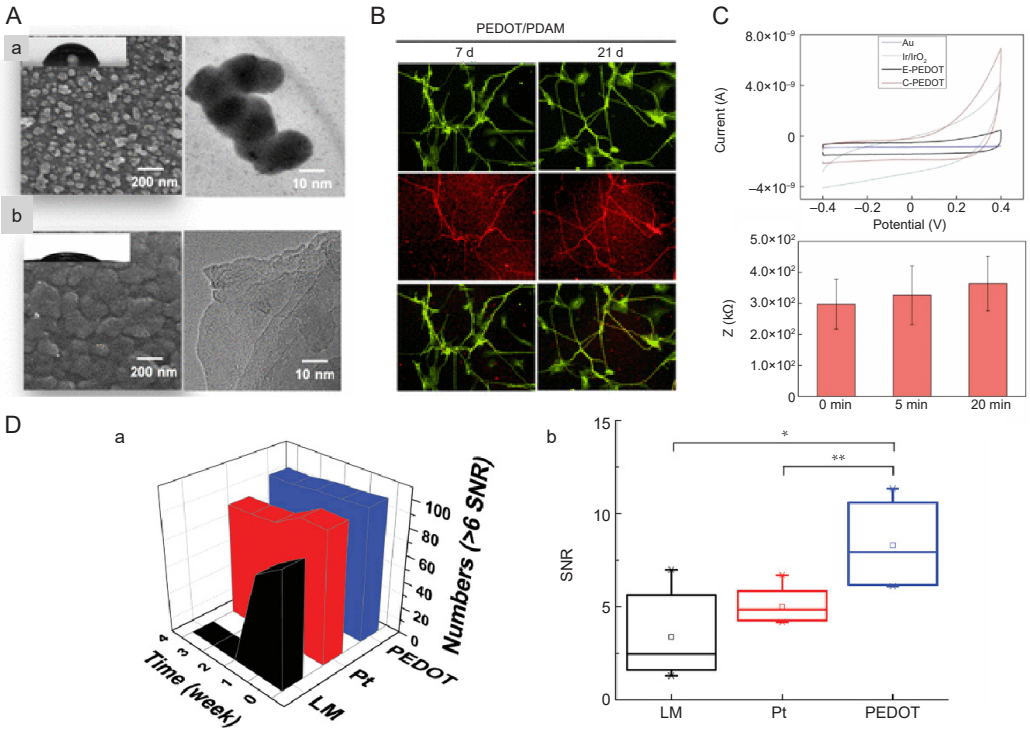

Figure 6. Conductive polymer material coatings for nerve electrodes. (A) SEM and TEM images of (a) PEDOT and (b) PEDOT/PDAM films. Scale bars: 200 nm (left), 10 nm (right). (B) Fluorescence images showing immunofluorescence staining of β-tubulin III (green), MAP2 (red), and nuclei (blue) after culturing neuronal progenitor cells in PEDOT/PDAM films for 21 days. (C) Cyclic voltammetry curves of chemically polymerised PEDOT and other interfaces (n = 3), impedance of electrodes at 20 kHz frequency after sonication. A–C were reprinted with permission from Huang et al.[130] Copyright 2022 American Chemical Society. (D) (a) The numbers of high-quality recording spikes (SNR > 6) of LM wire, Pt wire, and PEDOT LMEs for 4 weeks, and (b) analysis of variance test revealed the significant difference among the electrodes. *P < 0.05, **P < 0.01. D was reprinted from Lim et al.[133] Copyright 2022 Wiley-VCH GmbH. Reproduced with permission. Au: aurum; C-PEDOT: chemical polymerization PEDOT; E-PEDOT: electropolymerization PEDOT; Ir: iridium; IrO_3: iridium trioxide; LM: liquid metal; LME: liquid metal based electrode; MAP2: microtubule-associated protein 2; PDAM: 1-pyrenyldiazomethane; PEDOT: poly(3,4-ethylenedioxythiophene); Pt: platinum; SEM: scanning electron microscope; SNR: signal-to-noise ratio; TEM: transmission electron microscope.

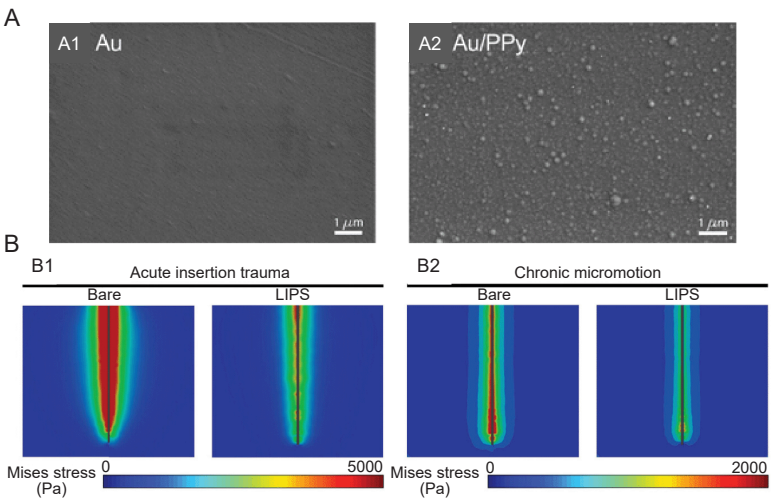

Figure 7. Coating with active substance grafts. (A) SEM images of (Aa) Au polyester film electrode and (A2) Au/PPy electrode surface. Reprinted with permission from Desroches et al.[138] Copyright 2020 American Chemical Society. (B) von Mises stress profiles of bare and LIPS-coated probes within brain tissue during insertion (B1) and under lateral micromotion of 100 μm (B2).[141] Au: aurum; LIPS: lubricated immune-stealthy probe surface; PPy: polypyrrole.

a variety of materials have been developed, a single material is often difficult to simultaneously meet the biological needs and electrical performance requirements. Combining different materials to prepare composite coatings is a common way to enhance the functionality of coatings.

Coatings made from metal and polymer materials are the most common composite coatings, and the excellent electrical conductivity of metals and the mechanical flexibility and biocompatibility of polymers can easily reach a mutual complementarity. Jain et al.[142] designed a Au wire electrode with a nanoparticle Au shell and a hydrogel layer, which achieved an effective electrical/ionic coupling between the hydrogel and the Au wire through the nanostructured Au shells on the surface of the Au wire (**Figure 8A**). Chen et al.[143] proposed a tissue-like metal-doped hydrogel, which could achieve excellent electrical biosensing by introducing disulfide-modified silver nanowires into a bifunctional hyaluronic acid/carboxymethyl chitosan composite. Plasma silver nanocubes were also introduced into polyacrylamide hydrogels in a similar manner to enhance the electrical properties of the system.[95] Carbon materials, as discussed previously, are also common neuroelectrode coating materials as both excellent electrical properties and biocompatible materials. However, carbon materials such as CNT, although generally considered to be non-cytotoxic to neuronal cells, their direct exposure in human tissues has also been suggested to lead to abnormal activation of immune cells,[144] and increased neuronal excitability induced by CNT can promote neuronal regeneration, but overexcitability may also lead to neurological damage.[145] For neuroelectrode materials applied to brain tissues, in order to pursue higher biocompatibility, the risk of carbon material application can be reduced by compositing with polymer hydrogels. Ye et al.[146] mixed CNT with ionic liquids to obtain reticulated CNTs and transferred them into hydrogel matrices by *in-situ* polymerisation of suitable monomers in ionic liquids, which were then converted into CNT-poly(ethylene glycol) hydrogel composites by solvent substitution. poly(ethylene glycol) hydrogel composite (**Figure 8B**). PC-12 cells cultured on this composite showed enhanced differentiation and increased neuronal to astrocyte ratio in neural stem cells. Another study prepared a multifunctional coating presenting both the anti-inflammatory drug dexamethasone and neuroprotective factor on top of multiwalled CNTs (MWCNTs) and PPy composite coatings (**Figure 8C**),[147] which was capable of releasing dexamethasone mediated by exogenous stimuli and effectively inhibiting inflammatory factor secretion and astrocyte proliferation. The charge storage capacitances of PPy/PSS and MWCNTs/dexamethasone-PPy/γ-poly(L-glutamic acid)/PSS-poly-L-lysine-nerve growth factor-modified electrodes were much larger than those of bare Au electrodes (**Figure 8D**). Among them, the capacitance change of MWCNTs/dexamethasone-PPy/γ-poly(L-glutamic acid)/PSS-poly-L-lysine-nerve growth factor-modified electrode was small, suggesting that drug loading in the CP may lead to weakening of the long-term stability of conductive coatings, whereas MWCNTs sandwiched between smooth electrodes and CPs enhance the stability of the coating materials, and thus the electrochemical performance.

Natural biomaterials have excellent biocompatibility and even bioactivity, but they are also often used in combination with conductive materials because they generally do not possess conductive properties. Wei et al.[148] prepared a novel multimodal transparent electrophysiological hydrogel, by freeze-thawing method using polyvinyl alcohol, quaternary ammonium chitosan, and hyaluronic acid (PVA@HACC@HA) as a polymer network. multimodal transparent electrophysiological hydrogel has a low modulus of elasticity (0.15 MPa) and can be conformably and tightly adhered to brain tissues (**Figure 8C**, and **D**) causing minimal immune response due to mechanical damage; conducts electricity through ions and has a low interfacial impedance with brain tissues (150 Ω at 1 kHz); and has a transmittance of 93% in the wavelength range of 300–1100 nm. Ding et al.[111] constructed a conductive hydrogel electrode material of filipin protein by chemically grafting tyramine monomers onto CNTs and simultaneously constructing a 3D covalent network between silk fibroin and CNTs, which enabled faster gelation of silk fibroin. The 3D covalent network has good electro-permeability properties, which enhances the conductivity of the hydrogel by promoting the movement of electrons at the interface of the neuroelectrode, and enables more effective recording of weak neuroelectric signals.

Coating Fabrication Techniques

A variety of coating preparation techniques have been applied to the fabrication of neural electrode coatings, while neural electrodes are often characterised by low mechanical strength and miniaturized dimensions, and need to be in long-term service in the human body, which also puts forward higher requirements for coating technology. In addition to ensuring the long-term stability of the connection between the coating material and the electrode, advanced coating technology should also support the internal structure of the coating as well as the controllable preparation of the surface morphology. Currently, technologies for the controlled fabrication of coatings with specific structures and patterns can be roughly categorised into subtractive manufacturing (photolithography, etching)[149-152] and additive manufacturing (chemical vapour deposition (CVD),[153-155] electrochemical deposition,[156-158] electrospinning,[159-161] and microcontact printing).[162-164] Using these techniques, it is possible to customise microscopic morphologies with specific geometric patterns, 3D structures, and roughness on electrode surfaces with different compositional structures and physicochemical properties at the micro (nano) metre scale.

Subtractive manufacturing

Photo-lithography, etching and laser ablation are common micro-fabrication processes that are now widely used for the preparation of micro-electrode arrays or other 3D electrode materials. Seo et al.[165] used photo-lithography to fabricate a high-density filamentary neuroelectrode array. 256 electrodes were integrated in a small area of 2300 × 300 μm^2, with each electrode site being only 34 × 7 μm^2. Using photomasks designed by complex patterns, Roh et al.[166] used photo-lithography and ion etching in conjunction to simplify the fabrication of MEAs with different heights and cross-sectional shapes.

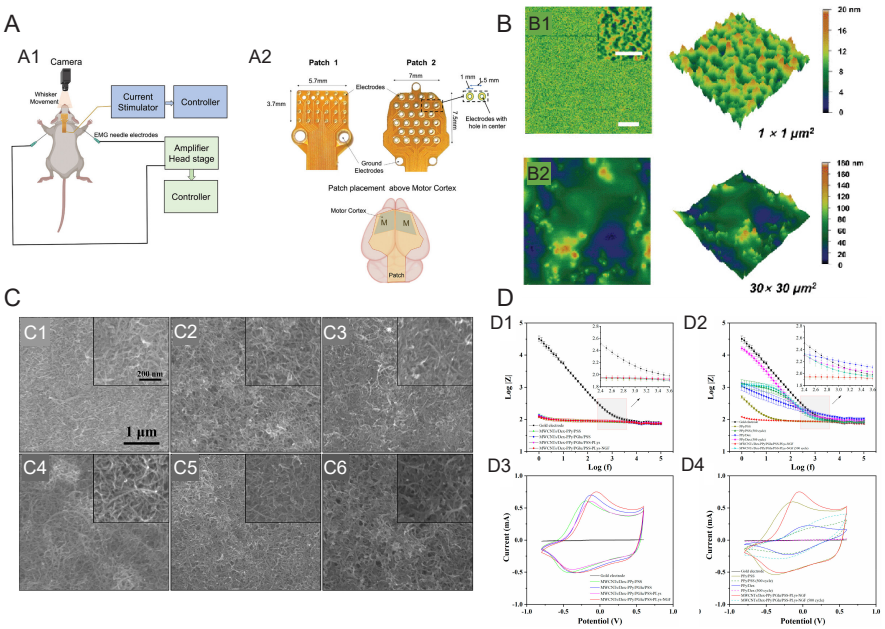

Figure 8. Neuroelectrodes with composite coatings. (A) (A1) Schematic representation of stimulation paradigm showing connection of the stimulation patch and EMG electrodes placement along with camera for whisker movement recording. (A2) Two different flexible patches were used for HD-ECS. Patch 1 contained 24 disk electrodes arranged in a 6 × 4 array in a cartesian grid, and Patch 2 had 27 ring-shaped electrodes arranged in a hexagonal grid. The patch was placed above the skull with its centre aligned to bregma, covering the motor cortex of both hemispheres.[142] (B) Surface morphology (2D and 3D height images) of c-PEG-0 (B1) and c-PEG-20 (B2) samples in water taken by AFM. Scale bars: 5 μm (inset: 500 nm).[146] (C) SEM images of different functional coatings. (C1) MWCNTs, (C2) MWCNTs/Dex-PPy/PSS, (C3) MWCNTs/Dex-PPy/PGlu/PSS, (C4) MWCNTs/Dex-PPy/PGlu/PSS-PLys, (C5) MWCNTs/Dex-PPy/PGlu/PSS-PLys-NGF (before CV stimulation), and (C6) MWCNTs/Dex-PPy/PGlu/PSS-PLys-NGF coatings (after 500 cycles of CV stimulation). Insets are corresponding images with higher magnification. (D) (D1, D3) EIS (D1) and CV (D3) of bare Au electrodes, MWCNTs/Dex-PPy/PSS, MWCNTs/Dex-PPy/PGlu/PSS, MWCNTs/Dex-PPy/PGlu/PSS-PLys, and MWCNTs/Dex-PPy/PGlu/PSS-PLys-NGF functional coatings. Comparison of EIS (D2) and CV (D4) of bare Au electrodes, PPy/PSS films, PPy/Dex films, and MWCNTs/Dex-PPy/PGlu/PSS-PLys-NGF functional coatings. Data are represented by mean ± standard deviation ($n \geq 3$). Reprinted with permission from Tian et al.[147] Copyright 2022 American Chemical Society. 2D: two dimensional; 3D: three dimensional; AFM: atomic force microscope; Au: aurum; c-PEG: carbon nanotube-poly(ethylene glycol); CV: cyclic voltammetry; Dex: dexamethasone; MWCNT: multiwalled carbon nanotube; NGF: nerve growth factor; PGlu: poly(glutamic acid); PLys: poly(lysine); PPy: polypyrrole; PSS: poly(styrene sulfonate); SEM: scanning electron microscope.

Compared to lithography, the fabrication of polymer masks (e.g. polyimide films) by laser ablation allows for simpler preparation of patterned macro molecular biomaterials or polymer coatings.[167] There have been numerous applications of laser technology for patterning neuroelectrode materials, including the use of lasers to cut and pattern metal electrodes,[168, 169] the use of laser melting to increase the electrode surface area,[170] and the improvement of the electrode surface electrochemical activity,[171] etc. Yang et al.[172] developed a patterning technique based on ultrafast pulsed laser ablation for the large-volume sequential fabrication of various groups of organic and inorganic degradable materials, with high resolution of coating patterns and the ability to prepare multilayer structures with precise superposition. Amini et al.[173] developed a new method of hierarchical surface restructuring of electrode surfaces using femtosecond laser technology, which significantly improved the electrical properties of Pt-Ir electrode surfaces. Won et al.[174] developed an ultrafast digital patterning process using a 3D-printing-like approach by laser-induced PEDOT:PSS phase separation, and the processed PEDOT:PSS has good water stability and can retain only the laser-patterned portion after water washing.

Additive manufacturing

CVD is widely used for the growth of carbon material coatings. Through the application of different catalyst lithography patterns, CVD-synthesised CNTs can be grown into highly porous mats or highly ordered and vertically aligned column bundles.[175] Highly porous CNTs with fluffy mat-like structures have a larger charge transfer surface area and preferential adhesion of nerve cells to CNTs via dendritic entanglement can significantly improve signal recording at nerve electrodes.[176] In addition to CVD-fabricated flexible graphene electrode arrays with low impedance and high signal-to-noise ratio,[177] multilayer graphene electrodes fabricated by CVD using a wafer-level no-transfer process exhibited very low impedance (4.1 kΩ) comparable to precious metal electrodes.[178]

Electrostatic spinning is another simple and highly versatile technique which is widely applicable in a variety of polymers

and composites and allows large-scale fabrication of continuous ultrafine fibres. Fibres manufactured by electrostatic spinning are known for high uniformity, high porosity, high surface area and high mechanical strength. Lee et al.[179] fabricated nanofibrous conductive scaffolds by deposition of nano-thick PPy on poly(lactic-co-glycolic acid) nanofibres using electrostatic spinning technique. Electrical stimulation of PC-12 cells on conductive PPy/poly(lactic-co-glycolic acid) nanofibre scaffolds was found to improve neurite growth compared to unstimulated cells.

Electrodeposition is a versatile coating technique that can be widely used for the preparation of coatings on metals, polymers, and natural biomaterials. By adjusting the electrochemical parameters of the deposition process, the structure and morphology of the coatings can be controllably altered during the deposition process. Mousavi et al.[180] investigated the relationship between the mechanical stability of the electro-polymerisation of PEDOT:PSS on substrate materials and the thickness of the coatings, the adhesive surface properties, and the parameters of the electrodeposition operation (applied voltage/current, duration, and number of repetitions). The results show that the morphology of the PEDOT:PSS coatings and their adhesion to the electrode surfaces mainly depend on the properties of the electrode surfaces themselves. PEDOT:PSS forms a cauliflower-like shape on carbon microfilament electrodes, but is smoother on flat half-in and Au microfilament electrodes. One of the major problems faced by electrodeposited PEDOT coatings is the mechanical stability between the coating and the electrode, problems such as cracking and peeling of the coating can greatly affect the service life of the electrode, in order to enhance the stability of PEDOT coatings, there have been a number of studies to improve on the electrodeposition technology. Zhang et al.[56] combined a functional long-chain polymer poly(styrenesulfonate-co-4-vinylpyridine) chemically grafted onto a metal substrate, followed by electrochemical deposition of PEDOT and chemical cross-linking to form a PEDOT:poly(styrenesulfonate-co-4-vinylpyridine) interpenetrating network. This integrated polymer chain anchoring and chemical cross-linking method enabled the conductive hydrogel coating and metal electrode substrate to exhibit excellent interfacial robustness under long-term charge/discharge cycling and strong mechanical ultrasonic treatments. Yang et al.[181] prepared poly(5-nitroindole) thin films by an electro-polymerisation and electro-grafting method as an Au/poly(5-nitroindole)/PEDOT conductive and adhesive interface layer for neural electrodes, which significantly enhanced the adhesion between PEDOT and Au electrode substrates (peel strength over 1.72 N/mm).

Structure Design of Coatings with Cellular Modulation Capabilities

Micromorphology regulates neuronal activity

Extracellular matrix not only provides nutrients for cells and regulates cell behaviours such as adhesion, growth, and differentiation through soluble biochemical signals, but also constitutes a growth environment for cells with complex physical parameters. It has been shown that a large number of cells, including neural cells, are affected by the physical parameters of the growth environment (e.g., microstructure, surface morphology, and mechanical strength) during their growth and development.[182-184]

From a previous study, the influence of microforms on cell growth comes from two main pathways:[185] i) direct influence on the cytoskeleton through mechanical signalling; ii) indirect influence on the cell through extracellular chemical signalling.

Adhesion molecules are a functional cellular mechanism by which cells recognise external physical environment, and topographical cues. This has been widely demonstrated in cells other than neuronal cells. Adhesion molecules are primarily based on integrin formation.[186] When integrins are activated by external mechanical features, they induce the assembly of focal adhension and cause integrins to attach to actin filaments of the cytoskeleton, leading to a change in cell shape.[187] In neuronal cells, integrins are also widely present, and the presence of integrins in neurons primarily affects neuronal migration and axonal growth. Another view is that surface morphology indirectly influences cellular activity by adsorbing proteins in the extracellular matrix.[188] In the usual culture process, cells often do not come into direct contact with the material, as the material tends to be encapsulated in a monolayer of adsorbed proteins in the supernatant first, and then comes into contact with the cells later. Thus, the host cell is not actually directly affected by the material, but by the surface proteins. Nanoscale surface morphology has different effects on the morphology and conformation of surface-bound proteins.

Micro-morphology design of nerve electrode coatings

There have been studies summarised the effects of different morphological cues on neuronal cell growth and development,[185, 189-191] such as groove structures with staggered cell/subcell widths can enhance the directional growth of neuronal cells along the direction of the grooves; discontinuous dots, columns, and cones bumps of cell/subcell dimensions can be oriented to neuronal and glial cells; and nanoscale random topographies can also affect the specific behaviour of nerve cells. The effects of microtopography on neuronal cells can be categorised mainly into cell adhesion, orientation guidance, and neurite growth.

Neurons, like other anchorage-dependent cells, require proper adhesion to substrates for growth and development, so enhancing the adhesion of neuronal cells on the surface of nerve electrodes by microtopography can promote neuronal cell growth. As shown in **Figure 9A**, an irregularly distributed structured Au surface mimicking natural collagen fibres,[192] with 1% decrease in impedance amplitude and 35% increase in critical free surface energy at frequencies lower than 50 kHz, improved the adhesion and growth of mouse enteric neuronal cells on its surface. Yang et al.[58] designed an electrode surface consisting of a conductive PEDOT:PSS network and a multifunctional polyazo-polyether-poly((sulfonyl) betaine) network to form a multifunctional hydrogel with semi-interpenetrating network. Since the polyazo-polyether-poly((sulfonyl) betaine) network can be covalently crosslinked by ultraviolet light triggering and constructed by photolithography with a high-resolution

pattern of 50 μm in both line and gap widths (**Figure 9B**), it possesses bio adhesive and antifouling properties.

The intimate contact and communication between neurons and electrodes determine the working efficiency of neural electrodes, and neurons, as special cells, have unique neural protrusion structures as carriers of electrical signals. The development and growth direction of the neurites on the electrode surface greatly affect the signal communication ability between the neuron and the electrode. Grooves or ridges of cellular/subcellular dimensions can guide the directional growth of neuronal synapses, biomimetic porous scaffold structures can guide neurons to form a network within the scaffolds, and such patterning of the electrode coatings can promote the tight connection between neurons and electrodes. Tringides et al.[193] prepared scaffolds that mimic the environment of neural tissue by doping carbon nanomaterials in alginate hydrogel matrix and freeze-drying them. The neural progenitor cells in the scaffolds were able to form neuronal networks that spanned the material in three dimensions and differentiated into astrocytes and myelinated oligodendrocytes, as shown in **Figure 9C**. Wang et al.[194] fabricated 3D conductive scaffolds based on printed microfibrous structures using near-field electrostatic printing and graphene oxide coating. Various ultrafine fibre patterns were obtained from poly(L-lactic-co-caprolactone) by near-field electrostatic printing, and the coverage angle of poly(L-lactic-co-caprolactone) fibres and fibre diameters were adjusted to construct spiderweb-like and tubular fibrous spatial tissues with complex spatial structures (**Figure 9D**, and **E**). This conductive scaffold showed excellent electrical conductivity (~0.95 S/cm) and was able to induce the formation of neuron-like networks in the scaffold under exogenous electrical stimulation.

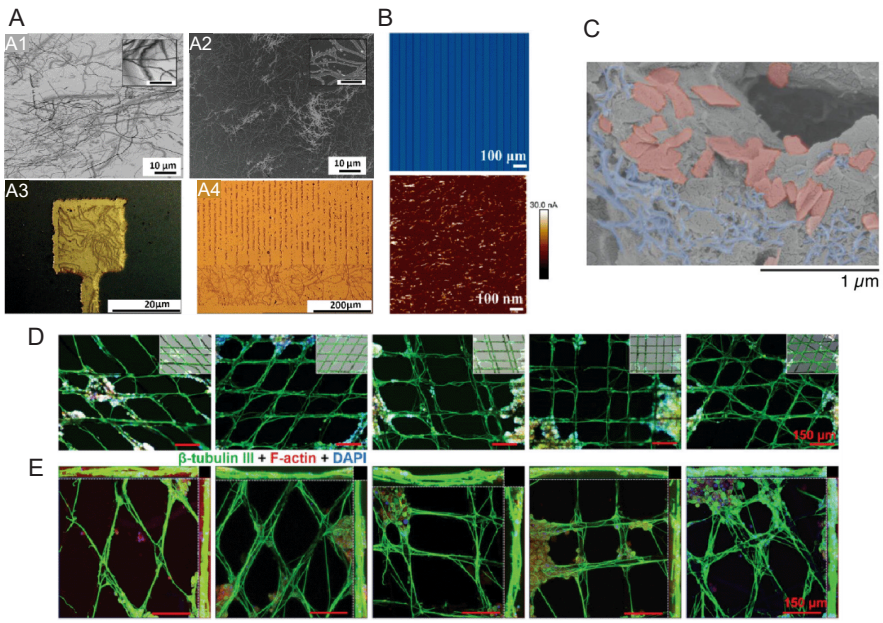

Figure 9. Neuroelectrode coatings for regulating cellular activity through microforms. (A) SEM images of (A1) collagen fibres coated on silicon wafer and (A2) collagen-like Au nanostructures developed from the nanoimprint process; Application of CLGNS nanostructuring process on (A3) microelectrode array surface and (A4) meander pattern, as proof of concept.[192] Scale bars: 10 μm (A1, A2), 20 μm (A3, A4) (inset scale bar 1 μm). (B) Photograph of photopatterned MH (15 wt% SBMA) and AFM current image of PEDOT:PSS treated with SBMA (15 wt%). Reprinted with permission from Yang et al.[58] Copyright 2023 American Chemical Society. (C) SEM micrographs of the scaffolds with alginate left gray, GF pseudo-colored red, and CNTs pseudo-colored blue. Scale bar: 1 μm. C was reprinted from Tringides et al.[193] Copyright 2023 Wiley-VCH GmbH. (D) Representative immunofluorescence images and (E) confocal microscopy images of PC-12 cells cultured on microfibres with different cladding angles for 14 days under ES conditions. Cultures were immunofluorescently stained with β-tubulin III (green), F-actin (red) and DAPI (blue). Inset: merged bright field images. D was reprinted from Wang et al.[194] Copyright 2020 Wiley-VCH GmbH. Scale bars: 150 μm. AFM: atomic force microscope; CLGNS: collagen-like gold nanostructure; DAPI: 4,6-diamidino-2-phenylindole; ES: electrical stimulation; MH: multifunctional hydrogel; PEDOT:PSS: poly(3,4-ethylenedioxythiophene):poly(styrene sulfonate); SBMA: 3-[dimethyl-[2-(2-methylprop-2-enoyloxy)ethyl] azaniumyl] propane-1-sulfonate; SEM: scanning electron microscope.

Conclusion and Prospect

The function of BCI in the acquisition and identification of neuroelectric signals and the application of reverse electrical stimulation is of great significance for the diagnosis of clinical diseases, the treatment of neurological related diseases, and the recovery of body functions. And the neuroelectrode, as the key part of physiological electrical signal acquisition in BCI, is of great significance for the development of BCI technology. This paper introduces the challenges faced by neuroelectrodes in applications and the key issues that need to be solved. Improvements in electrode substrate materials for neuroelectrode interfaces are highlighted from a

material design perspective, while recent advances in coating preparation techniques and structured design are discussed. Due to the huge difference between the fragile physiological structure of brain tissue and the external mechanical structure, the neuroelectrodes, as a "bridge" connecting the biological tissue and the external mechanical structure, need to satisfy the completely different functional requirements of the two ends at the same time, which has made the fabrication of neuroelectrodes always facing a great challenge.

Great progress has been made in the fabrication of neuroelectrodes, but there are still unresolved challenges that still require further attention. For implantable neuroelectrodes, biocompatibility is still the main issue. In addition to improvements in electrode structure, mechanical properties, and material selection, more attention should be paid to the role of the neuroimmune response during electrode implantation. This is because neuronal growth and glial scar formation not only affect the biosafety, but also directly affect the signal reception ability of the neuroelectrode. Secondly the long-term stability of the neuroelectrode needs to be further evaluated, e.g., it is necessary to assess the use of the electrode several years or more after implantation. In addition, the signal-to-noise ratio of the recorded electrophysiological signals needs to be further improved.

Although the ideal neuroelectrode is still a long way off, novel electrode materials and processing technologies have been introduced, such as nanometallic materials, semiconductor materials, carbon nanomaterials, CPs, and bio-based materials, which continue to open up the possibilities of neuroelectrode materials. A single material is difficult to meet the multiple needs of neuroelectrodes, and composite neuroelectrodes with multiple materials, or coating modification of the base electrode using a combination of different materials, can provide more comprehensive advantages than single-material electrodes, such as (i) higher electrical and optical properties, such as low impedance, low signal-to-noise ratio, and stimulation ability of exogenous signals; (ii) lower modulus of elasticity, better adhesion properties, and brain tissue tight fitting to avoid mechanical damage and slippage; (iii) better physicochemical stability, biocompatibility, and bioactivity. On this basis, the use of more advanced micromachining molding technology to fabricate electrodes with lower volume and more complex structure; higher resolution patterning or structured design of coatings, and the modulation of nerve cells through morphological cues provide another direction for the functionalization of nerve electrodes. The combination of multiple materials and the expansion of new synthetic processing processes are all expected to realize truly ideal neuroelectrodes that will achieve the goal of seamless BCIs and make significant contributions to the fields of clinical medicine, brain function analysis, and human-computer interaction.

This review provides a comprehensive overview of the research in neuroelectrode substrate materials and coating modification technologies in the last 5 years, but mainly focuses on representative advances and does not provide overall statistics and analyses. The field of neuroelectrodes involves a large number of materials, a wide range of classifications, and a long history of development, so the content of this review is limited and does not cover the long-term development trend.

Author contributions

YJ, ML, JZ conceptualised and designed the review; YJ drafted the manuscript; YJ, RC, XQ checked and revised the manuscript. All authors reviewed and approved the final version of the manuscript.

Financial support

The work was supported by the National Key Research and Development Program, No. 2021YFB3800800, the National Natural Science Foundation of China, Nos. 31922041, 32171341, 32301113, the 111 Project, No. B14018, the Science and Technology Innovation Project and Excellent Academic Leader Project of Shanghai Science and Technology Committee, Nos. 21S31901500, 21XD1421100, the National Postdoctoral Program for Innovative Talents, No. BX20230122, the Shanghai Sailing Program, No. 23YF1409700, and the China Postdoctoral Science Foundation, No. D100-5R-22114.

Acknowledgement

None.

Conflicts of interest statement

The authors declare no conflict of interest.

1. Serino, A.; Bockbrader, M.; Bertoni, T.; Colachis Iv, S.; Solcà, M.; Dunlap, C.; Eipel, K.; Ganzer, P.; Annetta, N.; Sharma, G.; Orepic, P.; Friedenberg, D.; Sederberg, P.; Faivre, N.; Rezai, A.; Blanke, O. Sense of agency for intracortical brain-machine interfaces. *Nat Hum Behav.* **2022**, *6*, 565-578.
2. Shanechi, M. M. Brain-machine interfaces from motor to mood. *Nat Neurosci.* **2019**, **22**, 1554-1564.
3. Young, M. J.; Lin, D. J.; Hochberg, L. R. Brain-Computer Interfaces in Neurorecovery and Neurorehabilitation. *Semin Neurol.* **2021**, *41*, 206-216.
4. Steins, H.; Mierzejewski, M.; Brauns, L.; Stumpf, A.; Kohler, A.; Heusel, G.; Corna, A.; Herrmann, T.; Jones, P. D.; Zeck, G.; von Metzen, R.; Stieglitz, T. A flexible protruding microelectrode array for neural interfacing in bioelectronic medicine. *Microsyst Nanoeng.* **2022**, *8*, 131.
5. Choi, J. S.; Lee, H. J.; Rajaraman, S.; Kim, D. H. Recent advances in three-dimensional microelectrode array technologies for in vitro and in vivo cardiac and neuronal interfaces. *Biosens Bioelectron.* **2021**, *171*, 112687.
6. Fattahi, P.; Yang, G.; Kim, G.; Abidian, M. R. A review of organic and inorganic biomaterials for neural interfaces. *Adv Mater.* **2014**, *26*, 1846-1885.
7. Cruz, A. M.; Casañ-Pastor, N. Graded conducting titanium–iridium oxide coatings for bioelectrodes in neural systems. *Thin Solid Films.* **2013**, *534*, 316-324.
8. Chapman, C. A.; Chen, H.; Stamou, M.; Biener, J.; Biener, M. M.; Lein, P. J.; Seker, E. Nanoporous gold as a neural interface coating: effects of topography, surface chemistry, and feature size. *ACS Appl Mater Interfaces.* **2015**, *7*, 7093-7100.
9. Boehler, C.; Stieglitz, T.; Asplund, M. Nanostructured platinum grass enables superior impedance reduction for neural microelectrodes. *Biomaterials.* **2015**, *67*, 346-353.
10. Li, J.; Cheng, Y.; Gu, M.; Yang, Z.; Zhan, L.; Du, Z. Sensing and stimulation applications of carbon nanomaterials in implantable brain-

computer interface. *Int J Mol Sci.* **2023**, *24*, 5182.

11. Kim, T.; Park, J.; Sohn, J.; Cho, D.; Jeon, S. Bioinspired, highly stretchable, and conductive dry adhesives based on 1D-2D hybrid carbon nanocomposites for all-in-one ECG electrodes. *ACS Nano.* **2016**, *10*, 4770-4778.
12. Kuzum, D.; Takano, H.; Shim, E.; Reed, J. C.; Juul, H.; Richardson, A. G.; de Vries, J.; Bink, H.; Dichter, M. A.; Lucas, T. H.; Coulter, D. A.; Cubukcu, E.; Litt, B. Transparent and flexible low noise graphene electrodes for simultaneous electrophysiology and neuroimaging. *Nat Commun.* **2014**, *5*, 5259.
13. Golparvar, A. J.; Yapici, M. K. Electrooculography by wearable graphene textiles. *IEEE Sens J.* **2018**, *18*, 8971-8978.
14. Apollo, N. V.; Maturana, M. I.; Tong, W.; Nayagam, D. A. X.; Shivdasani, M. N.; Foroughi, J.; Wallace, G. G.; Prawer, S.; Ibbotson, M. R.; Garrett, D. J. Soft, Flexible freestanding neural stimulation and recording electrodes fabricated from reduced graphene oxide. *Adv Funct Mater.* **2015**, *25*, 3551-3559.
15. Du, X.; Jiang, W.; Zhang, Y.; Qiu, J.; Zhao, Y.; Tan, Q.; Qi, S.; Ye, G.; Zhang, W.; Liu, N. Transparent and stretchable graphene electrode by intercalation doping for epidermal electrophysiology. *ACS Appl Mater Interfaces.* **2020**, *12*, 56361-56371.
16. Green, R.; Abidian, M. R. Conducting polymers for neural prosthetic and neural interface applications. *Adv Mater.* **2015**, *27*, 7620-7637.
17. Green, R. A.; Lovell, N. H.; Wallace, G. G.; Poole-Warren, L. A. Conducting polymers for neural interfaces: challenges in developing an effective long-term implant. *Biomaterials.* **2008**, *29*, 3393-3399.
18. Guo, L.; Ma, M.; Zhang, N.; Langer, R.; Anderson, D. G. Stretchable polymeric multielectrode array for conformal neural interfacing. *Adv Mater.* **2014**, *26*, 1427-1433.
19. Han, L.; Lu, X.; Wang, M.; Gan, D.; Deng, W.; Wang, K.; Fang, L.; Liu, K.; Chan, C. W.; Tang, Y.; Weng, L. T.; Yuan, H. A mussel-inspired conductive, self-adhesive, and self-healable tough hydrogel as cell stimulators and implantable bioelectronics. *Small.* **2017**, *13*, 1601916.
20. Kim, D. H.; Viventi, J.; Amsden, J. J.; Xiao, J.; Vigeland, L.; Kim, Y. S.; Blanco, J. A.; Panilaitis, B.; Frechette, E. S.; Contreras, D.; Kaplan, D. L.; Omenetto, F. G.; Huang, Y.; Hwang, K. C.; Zakin, M. R.; Litt, B.; Rogers, J. A. Dissolvable films of silk fibroin for ultrathin conformal bio-integrated electronics. *Nat Mater.* **2010**, *9*, 511-517.
21. Adewole, D. O.; Serruya, M. D.; Wolf, J. A.; Cullen, D. K. Bioactive neuroelectronic interfaces. *Front Neurosci.* **2019**, *13*, 269.
22. Chalmers, E.; Lee, H.; Zhu, C.; Liu, X. Increasing the conductivity and adhesion of polypyrrole hydrogels with electropolymerized polydopamine. *Chem Mater.* **2020**, *32*, 234-244.
23. Gajendiran, M.; Choi, J.; Kim, S. J.; Kim, K.; Shin, H.; Koo, H. J.; Kim, K. Conductive biomaterials for tissue engineering applications. *J Ind Eng Chem.* **2017**, *51*, 12-26.
24. Franze, K.; Janmey, P. A.; Guck, J. Mechanics in neuronal development and repair. *Annu Rev Biomed Eng.* **2013**, *15*, 227-251.
25. Budday, S.; Ovaert, T. C.; Holzapfel, G. A.; Steinmann, P.; Kuhl, E. Fifty shades of brain: a review on the mechanical testing and modeling of brain tissue. *Arch Comput Methods Eng.* **2020**, *27*, 1187-1230.
26. Betz, T.; Koch, D.; Lu, Y. B.; Franze, K.; Käs, J. A. Growth cones as soft and weak force generators. *Proc Natl Acad Sci U S A.* **2011**, *108*, 13420-13425.
27. Zamproni, L. N.; Mundim, M.; Porcionatto, M. A. Neurorepair and regeneration of the brain: a decade of bioscaffolds and engineered microtissue. *Front Cell Dev Biol.* **2021**, *9*, 649891.
28. Carnicer-Lombarte, A.; Chen, S. T.; Malliaras, G. G.; Barone, D. G. Foreign body reaction to implanted biomaterials and its impact in nerve neuroprosthetics. *Front Bioeng Biotechnol.* **2021**, *9*, 622524.
29. Michelson, N. J.; Vazquez, A. L.; Eles, J. R.; Salatino, J. W.; Purcell, E. K.; Williams, J. J.; Cui, X. T.; Kozai, T. D. Y. Multi-scale, multi-modal analysis uncovers complex relationship at the brain tissue-implant neural interface: new emphasis on the biological interface. *J Neural Eng.* **2018**, *15*, 033001.
30. Bennett, C.; Mohammed, F.; Álvarez-Ciara, A.; Nguyen, M. A.; Dietrich, W. D.; Rajguru, S. M.; Streit, W. J.; Prasad, A. Neuroinflammation, oxidative stress, and blood-brain barrier (BBB) disruption in acute Utah electrode array implants and the effect of deferoxamine as an iron chelator on acute foreign body response. *Biomaterials.* **2019**, *188*, 144-159.
31. Kozai, T. D.; Vazquez, A. L.; Weaver, C. L.; Kim, S. G.; Cui, X. T. In vivo two-photon microscopy reveals immediate microglial reaction to implantation of microelectrode through extension of processes. *J Neural Eng.* **2012**, *9*, 066001.
32. Wellman, S. M.; Cambi, F.; Kozai, T. D. The role of oligodendrocytes and their progenitors on neural interface technology: A novel perspective on tissue regeneration and repair. *Biomaterials.* **2018**, *183*, 200-217.
33. Biran, R.; Martin, D. C.; Tresco, P. A. Neuronal cell loss accompanies the brain tissue response to chronically implanted silicon microelectrode arrays. *Exp Neurol.* **2005**, *195*, 115-126.
34. Chen, K.; Wellman, S. M.; Yaxiaer, Y.; Eles, J. R.; Kozai, T. D. In vivo spatiotemporal patterns of oligodendrocyte and myelin damage at the neural electrode interface. *Biomaterials.* **2021**, *268*, 120526.
35. Savya, S. P.; Li, F.; Lam, S.; Wellman, S. M.; Stieger, K. C.; Chen, K.; Eles, J. R.; Kozai, T. D. Y. In vivo spatiotemporal dynamics of astrocyte reactivity following neural electrode implantation. *Biomaterials.* **2022**, *289*, 121784.
36. Kim, G. H.; Kim, K.; Nam, H.; Shin, K.; Choi, W.; Shin, J. H.; Lim, G. CNT-Au nanocomposite deposition on gold microelectrodes for improved neural recordings. *Sens Actuators B Chem.* **2017**, *252*, 152-158.
37. Yuan, X.; Hierlemann, A.; Frey, U. Extracellular recording of entire neural networks using a dual-mode microelectrode array with 19584 electrodes and high SNR. *IEEE J Solid-State Circuits.* **2021**, *56*, 2466-2475.
38. Lin, C. M.; Lee, Y. T.; Yeh, S. R.; Fang, W. Flexible carbon nanotubes electrode for neural recording. *Biosens Bioelectron.* **2009**, *24*, 2791-2797.
39. Sabetian, P.; Popovic, M. R.; Yoo, P. B. Optimizing the design of bipolar nerve cuff electrodes for improved recording of peripheral nerve activity. *J Neural Eng.* **2017**, *14*, 036015.
40. Díaz, D. R.; Carmona, F. J.; Palacio, L.; Ochoa, N. A.; Hernández, A.; Prádanos, P. Impedance spectroscopy and membrane potential analysis of microfiltration membranes. The influence of surface fractality. *Chem Eng Sci.* **2018**, *178*, 27-38.
41. Wellman, S. M.; Li, L.; Yaxiaer, Y.; McNamara, I.; Kozai, T. D. Y. Revealing spatial and temporal patterns of cell death, glial proliferation, and blood-brain barrier dysfunction around implanted intracortical neural interfaces. *Front Neurosci.* **2019**, *13*, 493.
42. Wellman, S. M.; Kozai, T. D. Y. In vivo spatiotemporal dynamics of NG2 glia activity caused by neural electrode implantation. *Biomaterials.* **2018**, *164*, 121-133.
43. Camuñas-Mesa, L. A.; Quiroga, R. Q. A detailed and fast model of extracellular recordings. *Neural Comput.* **2013**, *25*, 1191-1212.
44. Kozai, T. D.; Langhals, N. B.; Patel, P. R.; Deng, X.; Zhang, H.; Smith, K. L.; Lahann, J.; Kotov, N. A.; Kipke, D. R. Ultrasmall implantable composite microelectrodes with bioactive surfaces for chronic neural

interfaces. *Nat Mater.* **2012**, *11*, 1065-1073.
45. Lee, H. C.; Ejserholm, F.; Gaire, J.; Currlin, S.; Schouenborg, J.; Wallman, L.; Bengtsson, M.; Park, K.; Otto, K. J. Histological evaluation of flexible neural implants; flexibility limit for reducing the tissue response? *J Neural Eng.* **2017**, *14*, 036026.
46. Seymour, J. P.; Kipke, D. R. Neural probe design for reduced tissue encapsulation in CNS. *Biomaterials.* **2007**, *28*, 3594-3607.
47. Kuo, J. T.; Kim, B. J.; Hara, S. A.; Lee, C. D.; Gutierrez, C. A.; Hoang, T. Q.; Meng, E. Novel flexible parylene neural probe with 3D sheath structure for enhancing tissue integration. *Lab Chip.* **2013**, *13*, 554-561.
48. Gao, K.; Li, G.; Liao, L.; Cheng, J.; Zhao, J.; Xu, Y. Fabrication of flexible microelectrode arrays integrated with microfluidic channels for stable neural interfaces. *Sens Actuators A Phys.* **2013**, *197*, 9-14.
49. Du, Z. J.; Kolarcik, C. L.; Kozai, T. D. Y.; Luebben, S. D.; Sapp, S. A.; Zheng, X. S.; Nabity, J. A.; Cui, X. T. Ultrasoft microwire neural electrodes improve chronic tissue integration. *Acta Biomater.* **2017**, *53*, 46-58.
50. Hong, G.; Lieber, C. M. Novel electrode technologies for neural recordings. *Nat Rev Neurosci.* **2019**, *20*, 330-345.
51. Zhu, M.; Wang, H.; Li, S.; Liang, X.; Zhang, M.; Dai, X.; Zhang, Y. Flexible electrodes for in vivo and in vitro electrophysiological signal recording. *Adv Healthc Mater.* **2021**, *10*, e2100646.
52. Hu, Z.; Niu, Q.; Hsiao, B. S.; Yao, X.; Zhang, Y. Bioactive polymer-enabled conformal neural interface and its application strategies. *Mater Horiz.* **2023**, *10*, 808-828.
53. Potter-Baker, K. A.; Nguyen, J. K.; Kovach, K. M.; Gitomer, M. M.; Srail, T. W.; Stewart, W. G.; Skousen, J. L.; Capadona, J. R. Development of superoxide dismutase mimetic surfaces to reduce accumulation of reactive oxygen species for neural interfacing applications. *J Mater Chem B.* **2014**, *2*, 2248-2258.
54. Zheng, X. S.; Snyder, N. R.; Woeppel, K.; Barengo, J. H.; Li, X.; Eles, J.; Kolarcik, C. L.; Cui, X. T. A superoxide scavenging coating for improving tissue response to neural implants. *Acta Biomater.* **2019**, *99*, 72-83.
55. Golabchi, A.; Wu, B.; Li, X.; Carlisle, D. L.; Kozai, T. D. Y.; Friedlander, R. M.; Cui, X. T. Melatonin improves quality and longevity of chronic neural recording. *Biomaterials.* **2018**, *180*, 225-239.
56. Zhang, J.; Wang, L.; Xue, Y.; Lei, I. M.; Chen, X.; Zhang, P.; Cai, C.; Liang, X.; Lu, Y.; Liu, J. Engineering electrodes with robust conducting hydrogel coating for neural recording and modulation. *Adv Mater.* **2023**, *35*, e2209324.
57. Yuk, H.; Lu, B.; Zhao, X. Hydrogel bioelectronics. *Chem Soc Rev.* **2019**, *48*, 1642-1667.
58. Yang, M.; Chen, P.; Qu, X.; Zhang, F.; Ning, S.; Ma, L.; Yang, K.; Su, Y.; Zang, J.; Jiang, W.; Yu, T.; Dong, X.; Luo, Z. Robust neural interfaces with photopatternable, bioadhesive, and highly conductive hydrogels for stable chronic neuromodulation. *ACS Nano.* **2023**. doi: 10.1021/acsnano.2c04606.
59. Wu, Z. Z.; Zhao, Y.; Kisaalita, W. S. Interfacing SH-SY5Y human neuroblastoma cells with SU-8 microstructures. *Colloids Surf B Biointerfaces.* **2006**, *52*, 14-21.
60. Fan, Y. W.; Cui, F. Z.; Hou, S. P.; Xu, Q. Y.; Chen, L. N.; Lee, I. S. Culture of neural cells on silicon wafers with nano-scale surface topograph. *J Neurosci Methods.* **2002**, *120*, 17-23.
61. Kushwah, N.; Woeppel, K.; Dhawan, V.; Shi, D.; Cui, X. T. Effects of neuronal cell adhesion molecule L1 and nanoparticle surface modification on microglia. *Acta Biomater.* **2022**, *149*, 273-286.
62. Woeppel, K. M.; Cui, X. T. Nanoparticle and biomolecule surface modification synergistically increases neural electrode recording yield and minimizes inflammatory host response. *Adv Healthc Mater.* **2021**, *10*, e2002150.
63. Sikder, M. K. U.; Tong, W.; Pingle, H.; Kingshott, P.; Needham, K.; Shivdasani, M. N.; Fallon, J. B.; Seligman, P.; Ibbotson, M. R.; Prawer, S.; Garrett, D. J. Laminin coated diamond electrodes for neural stimulation. *Mater Sci Eng C Mater Biol Appl.* **2021**, *118*, 111454.
64. Chou, N.; Byun, D.; Kim, S. MEMS-based microelectrode technologies capable of penetrating neural tissues. *Biomed Eng Lett.* **2014**, *4*, 109-119.
65. Trevathan, J. K.; Baumgart, I. W.; Nicolai, E. N.; Gosink, B. A.; Asp, A. J.; Settell, M. L.; Polaconda, S. R.; Malerick, K. D.; Brodnick, S. K.; Zeng, W.; Knudsen, B. E.; McConico, A. L.; Sanger, Z.; Lee, J. H.; Aho, J. M.; Suminski, A. J.; Ross, E. K.; Lujan, J. L.; Weber, D. J.; Williams, J. C.; Franke, M.; Ludwig, K. A.; Shoffstall, A. J. An injectable neural stimulation electrode made from an in-body curing polymer/metal composite. *Adv Healthc Mater.* **2019**, *8*, e1900892.
66. Patel, P. R.; Zhang, H.; Robbins, M. T.; Nofar, J. B.; Marshall, S. P.; Kobylarek, M. J.; Kozai, T. D.; Kotov, N. A.; Chestek, C. A. Chronic in vivo stability assessment of carbon fiber microelectrode arrays. *J Neural Eng.* **2016**, *13*, 066002.
67. Hong, W.; Lee, J. W.; Kim, D.; Hwang, Y.; Lee, J.; Kim, J.; Hong, N.; Kwon, H. J.; Jang, J. E.; Punga, A. R.; Kang, H. Ultrathin gold microelectrode array using polyelectrolyte multilayers for flexible and transparent electro-optical neural interfaces. *Adv Funct Mater.* **2022**, *32*, 2106493.
68. Lim, C.; Park, C.; Sunwoo, S. H.; Kim, Y. G.; Lee, S.; Han, S. I.; Kim, D.; Kim, J. H.; Kim, D. H.; Hyeon, T. Facile and scalable synthesis of whiskered gold nanosheets for stretchable, conductive, and biocompatible nanocomposites. *ACS Nano.* **2022**, *16*, 10431-10442.
69. Dong, R.; Wang, L.; Hang, C.; Chen, Z.; Liu, X.; Zhong, L.; Qi, J.; Huang, Y.; Liu, S.; Wang, L.; Lu, Y.; Jiang, X. Printed stretchable liquid metal electrode arrays for in vivo neural recording. *Small.* **2021**, *17*, e2006612.
70. Guo, R.; Liu, J. Implantable liquid metal-based flexible neural microelectrode array and its application in recovering animal locomotion functions. *J Micromech Microeng.* **2017**, *27*, 104002.
71. Zhang, X.; Liu, B.; Gao, J.; Lang, Y.; Lv, X.; Deng, Z.; Gui, L.; Liu, J.; Tang, R.; Li, L. Liquid metal-based electrode array for neural signal recording. *Bioengineering (Basel).* **2023**, *10*, 578.
72. Tang, R.; Zhang, C.; Liu, B.; Jiang, C.; Wang, L.; Zhang, X.; Huang, Q.; Liu, J.; Li, L. Towards an artificial peripheral nerve: Liquid metal-based fluidic cuff electrodes for long-term nerve stimulation and recording. *Biosens Bioelectron.* **2022**, *216*, 114600.
73. Kim, D.; Thissen, P.; Viner, G.; Lee, D. W.; Choi, W.; Chabal, Y. J.; Lee, J. B. Recovery of nonwetting characteristics by surface modification of gallium-based liquid metal droplets using hydrochloric acid vapor. *ACS Appl Mater Interfaces.* **2013**, *5*, 179-185.
74. So, J. H.; Koo, H. J.; Dickey, M. D.; Velev, O. D. Ionic current rectification in soft-matter diodes with liquid-metal electrodes. *Adv Funct Mater.* **2012**, *22*, 625-631.
75. Lee, S. H.; Thunemann, M.; Lee, K.; Cleary, D. R.; Tonsfeldt, K. J.; Oh, H.; Azzazy, F.; Tchoe, Y.; Bourhis, A. M.; Hossain, L.; Ro, Y. G.; Tanaka, A.; Kılıç, K.; Devor, A.; Dayeh, S. A. Scalable thousand channel penetrating microneedle arrays on flex for multimodal and large area coverage brainmachine interfaces. *Adv Funct Mater.* **2022**, *32*, 2112045.
76. Suzuki, I.; Matsuda, N.; Han, X.; Noji, S.; Shibata, M.; Nagafuku, N.; Ishibashi, Y. Large-area field potential imaging having single neuron resolution using 236 880 electrodes CMOS-MEA technology. *Adv Sci*

(Weinh). **2023**, *10*, e2207732.
77. Li, S.; Shi, Q.; Li, Y.; Yang, J.; Chang, T. H.; Jiang, J.; Chen, P. Y. Intercalation of metal ions into Ti3C2Tx MXene electrodes for high-areal-capacitance microsupercapacitors with neutral multivalent electrolytes. *Adv Funct Mater.* **2020**, *30*, 2003721.
78. Rafieerad, A.; Amiri, A.; Sequiera, G. L.; Yan, W.; Chen, Y.; Polycarpou, A. A.; Dhingra, S. Development of fluorine-free tantalum carbide MXene hybrid structure as a biocompatible material for supercapacitor electrodes. *Adv Funct Mater.* **2021**, *31*, 2100015.
79. Zhang, Y.; Zhang, L.; Li, C.; Han, J.; Huang, W.; Zhou, J.; Yang, Y. Hydrophilic antifouling 3D porous MXene/holey graphene nanocomposites for electrochemical determination of dopamine. *Microchem J.* **2022**, *181*, 107713.
80. Xu, J.; Shirinkami, H.; Hwang, S.; Jeong, H. S.; Kim, G.; Jun, S. B.; Chun, H. Fast reconfigurable electrode array based on titanium oxide for localized stimulation of cultured neural network. *ACS Appl Mater Interfaces.* **2023**, *15*, 19092-19101.
81. Zhang, F.; Zhang, L.; Xia, J.; Zhao, W.; Dong, S.; Ye, Z.; Pan, G.; Luo, J.; Zhang, S. Multimodal electrocorticogram active electrode array based on zinc oxide-thin film transistors. *Adv Sci (Weinh).* **2023**, *10*, e2204467.
82. Liu, S.; Liu, L.; Zhao, Y.; Wang, Y.; Wu, Y.; Zhang, X. D.; Ming, D. A high-performance electrode based on van der waals heterostructure for neural recording. *Nano Lett.* **2022**, *22*, 4400-4409.
83. Park, D. W.; Brodnick, S. K.; Ness, J. P.; Atry, F.; Krugner-Higby, L.; Sandberg, A.; Mikael, S.; Richner, T. J.; Novello, J.; Kim, H.; Baek, D. H.; Bong, J.; Frye, S. T.; Thongpang, S.; Swanson, K. I.; Lake, W.; Pashaie, R.; Williams, J. C.; Ma, Z. Fabrication and utility of a transparent graphene neural electrode array for electrophysiology, in vivo imaging, and optogenetics. *Nat Protoc.* **2016**, *11*, 2201-2222.
84. Park, S. Y.; Park, J.; Sim, S. H.; Sung, M. G.; Kim, K. S.; Hong, B. H.; Hong, S. Enhanced differentiation of human neural stem cells into neurons on graphene. *Adv Mater.* **2011**, *23*, H263-267.
85. Liu, X.; Xu, Z.; Fu, X.; Liu, Y.; Jia, H.; Yang, Z.; Zhang, J.; Wei, S.; Duan, X. Stable, long-term single-neuronal recording from the rat spinal cord with flexible carbon nanotube fiber electrodes. *J Neural Eng.* **2022**, *19*, 056024.
86. Yang, H.; Qian, Z.; Wang, J.; Feng, J.; Tang, C.; Wang, L.; Guo, Y.; Liu, Z.; Yang, Y.; Zhang, K.; Chen, P.; Sun, X.; Peng, H. Carbon nanotube array-based flexible multifunctional electrodes to record electrophysiology and ions on the cerebral cortex in real time. *Adv Funct Mater.* **2022**, *32*, 2204794.
87. Xiong, Z.; Huang, W.; Liang, Q.; Cao, Y.; Liu, S.; He, Z.; Zhang, R.; Zhang, B.; Green, R.; Zhang, S.; Li, D. Harnessing the 2D structure-enabled viscoelasticity of graphene-based hydrogel membranes for chronic neural interfacing. *Small Methods.* **2022**, *6*, e2200022.
88. Yang, X.; Zhu, J.; Qiu, L.; Li, D. Bioinspired effective prevention of restacking in multilayered graphene films: towards the next generation of high-performance supercapacitors. *Adv Mater.* **2011**, *23*, 2833-2838.
89. Xiong, J.; Zhang, B.; Balilonda, A.; Yang, S.; Li, K.; Zhang, Q.; Li, Y.; Wang, H.; Hou, C. Graphene-based implantable neural electrodes for insect flight control. *J Mater Chem B.* **2022**, *10*, 4632-4639.
90. Goding, J.; Gilmour, A.; Martens, P.; Poole-Warren, L.; Green, R. Interpenetrating conducting hydrogel materials for neural interfacing electrodes. *Adv Healthc Mater.* **2017**, *6*, 1601177.
91. Tomaskovic-Crook, E.; Zhang, P.; Ahtiainen, A.; Kaisvuo, H.; Lee, C. Y.; Beirne, S.; Aqrawe, Z.; Svirskis, D.; Hyttinen, J.; Wallace, G. G.; Travas-Sejdic, J.; Crook, J. M. Human neural tissues from neural stem cells using conductive biogel and printed polymer microelectrode arrays for 3D electrical stimulation. *Adv Healthc Mater.* **2019**, *8*, e1900425.
92. Widge, A. S.; Jeffries-El, M.; Cui, X.; Lagenaur, C. F.; Matsuoka, Y. Self-assembled monolayers of polythiophene conductive polymers improve biocompatibility and electrical impedance of neural electrodes. *Biosens Bioelectron.* **2007**, *22*, 1723-1732.
93. Liang, Q.; Shen, Z.; Sun, X.; Yu, D.; Liu, K.; Mugo, S. M.; Chen, W.; Wang, D.; Zhang, Q. Electron conductive and transparent hydrogels for recording brain neural signals and neuromodulation. *Adv Mater.* **2023**, *35*, e2211159.
94. Xia, X.; Liang, Q.; Sun, X.; Yu, D.; Huang, X.; Mugo, S. M.; Chen, W.; Wang, D.; Zhang, Q. Intrinsically electron conductive, antibacterial, and anti-swelling hydrogels as implantable sensors for bioelectronics. *Adv Funct Mater.* **2022**, *32*, 2208024.
95. Rinoldi, C.; Ziai, Y.; Zargarian, S. S.; Nakielski, P.; Zembrzycki, K.; Haghighat Bayan, M. A.; Zakrzewska, A. B.; Fiorelli, R.; Lanzi, M.; Kostrzewska-Księżyk, A.; Czajkowski, R.; Kublik, E.; Kaczmarek, L.; Pierini, F. In vivo chronic brain cortex signal recording based on a soft conductive hydrogel biointerface. *ACS Appl Mater Interfaces.* **2023**, *15*, 6283-6296.
96. Won, C.; Jeong, U. J.; Lee, S.; Lee, M.; Kwon, C.; Cho, S.; Yoon, K.; Lee, S.; Chun, D.; Cho, I. J.; Lee, T. Mechanically tissue-like and highly conductive au nanoparticles embedded elastomeric fiber electrodes of brain–machine interfaces for chronic in vivo brain neural recording. *Adv Funct Mater.* **2022**, *32*, 2205145.
97. Carli, S.; Bianchi, M.; Zucchini, E.; Di Lauro, M.; Prato, M.; Murgia, M.; Fadiga, L.; Biscarini, F. Electrodeposited PEDOT:nafion composite for neural recording and stimulation. *Adv Healthc Mater.* **2019**, *8*, e1900765.
98. Mandal, H. S.; Knaack, G. L.; Charkhkar, H.; McHail, D. G.; Kastee, J. S.; Dumas, T. C.; Peixoto, N.; Rubinson, J. F.; Pancrazio, J. J. Improving the performance of poly(3,4-ethylenedioxythiophene) for brain-machine interface applications. *Acta Biomater.* **2014**, *10*, 2446-2454.
99. Pranti, A. S.; Schander, A.; Bödecker, A.; Lang, W. PEDOT: PSS coating on gold microelectrodes with excellent stability and high charge injection capacity for chronic neural interfaces. *Sens Actuators B Chem.* **2018**, *275*, 382-393.
100. Liu, Y.; Liu, J.; Chen, S.; Lei, T.; Kim, Y.; Niu, S.; Wang, H.; Wang, X.; Foudeh, A. M.; Tok, J. B.; Bao, Z. Soft and elastic hydrogel-based microelectronics for localized low-voltage neuromodulation. *Nat Biomed Eng.* **2019**, *3*, 58-68.
101. Lu, B.; Yuk, H.; Lin, S.; Jian, N.; Qu, K.; Xu, J.; Zhao, X. Pure PEDOT:PSS hydrogels. *Nat Commun.* **2019**, *10*, 1043.
102. Feig, V. R.; Tran, H.; Lee, M.; Bao, Z. Mechanically tunable conductive interpenetrating network hydrogels that mimic the elastic moduli of biological tissue. *Nat Commun.* **2018**, *9*, 2740.
103. Li, T. L.; Liu, Y.; Forro, C.; Yang, X.; Beker, L.; Bao, Z.; Cui, B.; Paşca, S. P. Stretchable mesh microelectronics for the biointegration and stimulation of human neural organoids. *Biomaterials.* **2022**, *290*, 121825.
104. Wang, S.; Guan, S.; Wang, J.; Liu, H.; Liu, T.; Ma, X.; Cui, Z. Fabrication and characterization of conductive poly (3,4-ethylenedioxythiophene) doped with hyaluronic acid/poly (l-lactic acid) composite film for biomedical application. *J Biosci Bioeng.* **2017**, *123*, 116-125.
105. Ohm, Y.; Pan, C.; Ford, M. J.; Huang, X.; Liao, J.; Majidi, C. An electrically conductive silver–polyacrylamide–alginate hydrogel composite for soft electronics. *Nat Electron.* **2021**, *4*, 185-192.
106. Alizadeh, R.; Zarrintaj, P.; Kamrava, S. K.; Bagher, Z.; Farhadi, M.; Heidari, F.; Komeili, A.; Gutiérrez, T. J.; Saeb, M. R. Conductive

hydrogels based on agarose/alginate/chitosan for neural disorder therapy. *Carbohydr Polym.* **2019**, *224*, 115161.
107. Mili, B.; Das, K.; Kumar, A.; Saxena, A. C.; Singh, P.; Ghosh, S.; Bag, S. Preparation of NGF encapsulated chitosan nanoparticles and its evaluation on neuronal differentiation potentiality of canine mesenchymal stem cells. *J Mater Sci Mater Med.* **2017**, *29*, 4.
108. Qasim, S. B.; Zafar, M. S.; Najeeb, S.; Khurshid, Z.; Shah, A. H.; Husain, S.; Rehman, I. U. Electrospinning of chitosan-based solutions for tissue engineering and regenerative medicine. *Int J Mol Sci.* **2018**, *19*, 407.
109. Aznar-Cervantes, S.; Pagán, A.; Martínez, J. G.; Bernabeu-Esclapez, A.; Otero, T. F.; Meseguer-Olmo, L.; Paredes, J. I.; Cenis, J. L. Electrospun silk fibroin scaffolds coated with reduced graphene promote neurite outgrowth of PC-12 cells under electrical stimulation. *Mater Sci Eng C Mater Biol Appl.* **2017**, *79*, 315-325.
110. Cui, Y.; Zhang, F.; Chen, G.; Yao, L.; Zhang, N.; Liu, Z.; Li, Q.; Zhang, F.; Cui, Z.; Zhang, K.; Li, P.; Cheng, Y.; Zhang, S.; Chen, X. A stretchable and transparent electrode based on PEGylated silk fibroin for in vivo dual-modal neural-vascular activity probing. *Adv Mater.* **2021**, *33*, e2100221.
111. Ding, J.; Chen, Z.; Liu, X.; Tian, Y.; Jiang, J.; Qiao, Z.; Zhang, Y.; Xiao, Z.; Wei, D.; Sun, J.; Luo, F.; Zhou, L.; Fan, H. A mechanically adaptive hydrogel neural interface based on silk fibroin for high-efficiency neural activity recording. *Mater Horiz.* **2022**, *9*, 2215-2225.
112. Cho, Y.; Borgens, R. B. The effect of an electrically conductive carbon nanotube/collagen composite on neurite outgrowth of PC12 cells. *J Biomed Mater Res A.* **2010**, *95*, 510-517.
113. Liu, X.; Yue, Z.; Higgins, M. J.; Wallace, G. G. Conducting polymers with immobilised fibrillar collagen for enhanced neural interfacing. *Biomaterials.* **2011**, *32*, 7309-7317.
114. Yue, Z.; Liu, X.; Molino, P. J.; Wallace, G. G. Bio-functionalisation of polydimethylsiloxane with hyaluronic acid and hyaluronic acid--collagen conjugate for neural interfacing. *Biomaterials.* **2011**, *32*, 4714-4724.
115. Dhawan, V.; Cui, X. T. Carbohydrate based biomaterials for neural interface applications. *J Mater Chem B.* **2022**, *10*, 4714-4740.
116. Zhou, Y.; Gu, C.; Liang, J.; Zhang, B.; Yang, H.; Zhou, Z.; Li, M.; Sun, L.; Tao, T. H.; Wei, X. A silk-based self-adaptive flexible opto-electro neural probe. *Microsyst Nanoeng.* **2022**, *8*, 118.
117. Yang, J.; Du, M.; Wang, L.; Li, S.; Wang, G.; Yang, X.; Zhang, L.; Fang, Y.; Zheng, W.; Yang, G.; Jiang, X. Bacterial cellulose as a supersoft neural interfacing substrate. *ACS Appl Mater Interfaces.* **2018**, *10*, 33049-33059.
118. Potter-Baker, K. A.; Stewart, W. G.; Tomaszewski, W. H.; Wong, C. T.; Meador, W. D.; Ziats, N. P.; Capadona, J. R. Implications of chronic daily anti-oxidant administration on the inflammatory response to intracortical microelectrodes. *J Neural Eng.* **2015**, *12*, 046002.
119. Golabchi, A.; Woeppel, K. M.; Li, X.; Lagenaur, C. F.; Cui, X. T. Neuroadhesive protein coating improves the chronic performance of neuroelectronics in mouse brain. *Biosens Bioelectron.* **2020**, *155*, 112096.
120. Azemi, E.; Lagenaur, C. F.; Cui, X. T. The surface immobilization of the neural adhesion molecule L1 on neural probes and its effect on neuronal density and gliosis at the probe/tissue interface. *Biomaterials.* **2011**, *32*, 681-692.
121. Oakes, R. S.; Polei, M. D.; Skousen, J. L.; Tresco, P. A. An astrocyte derived extracellular matrix coating reduces astrogliosis surrounding chronically implanted microelectrode arrays in rat cortex. *Biomaterials.* **2018**, *154*, 1-11.
122. Vitale, F.; Shen, W.; Driscoll, N.; Burrell, J. C.; Richardson, A. G.; Adewole, O.; Murphy, B.; Ananthakrishnan, A.; Oh, H.; Wang, T.; Lucas, T. H.; Cullen, D. K.; Allen, M. G.; Litt, B. Biomimetic extracellular matrix coatings improve the chronic biocompatibility of microfabricated subdural microelectrode arrays. *PLoS One.* **2018**, *13*, e0206137.
123. Ramesh, V.; Stratmann, N.; Schaufler, V.; Angelov, S. D.; Nordhorn, I. D.; Heissler, H. E.; Martínez-Hincapié, R.; Čolić, V.; Rehbock, C.; Schwabe, K.; Karst, U.; Krauss, J. K.; Barcikowski, S. Mechanical stability of nano-coatings on clinically applicable electrodes, generated by electrophoretic deposition. *Adv Healthc Mater.* **2022**, *11*, e2102637.
124. Ramesh, V.; Rehbock, C.; Giera, B.; Karnes, J. J.; Forien, J. B.; Angelov, S. D.; Schwabe, K.; Krauss, J. K.; Barcikowski, S. Comparing direct and pulsed-direct current electrophoretic deposition on neural electrodes: deposition mechanism and functional influence. *Langmuir.* **2021**. doi: 10.1021/acs.langmuir.1c01081.
125. Angelov, S. D.; Koenen, S.; Jakobi, J.; Heissler, H. E.; Alam, M.; Schwabe, K.; Barcikowski, S.; Krauss, J. K. Electrophoretic deposition of ligand-free platinum nanoparticles on neural electrodes affects their impedance in vitro and in vivo with no negative effect on reactive gliosis. *J Nanobiotechnology.* **2016**, *14*, 3.
126. Yang, D.; Tian, G.; Liang, C.; Yang, Z.; Zhao, Q.; Chen, J.; Ma, C.; Jiang, Y.; An, N.; Liu, Y.; Qi, D. Double-microcrack coupling stretchable neural electrode for electrophysiological communication. *Adv Funct Mater.* **2023**, *33*, 2300412.
127. Nguyen, T. K.; Barton, M.; Ashok, A.; Truong, T. A.; Yadav, S.; Leitch, M.; Nguyen, T. V.; Kashaninejad, N.; Dinh, T.; Hold, L.; Yamauchi, Y.; Nguyen, N. T.; Phan, H. P. Wide bandgap semiconductor nanomembranes as a long-term biointerface for flexible, implanted neuromodulator. *Proc Natl Acad Sci U S A.* **2022**, *119*, e2203287119.
128. Dong, M.; Coleman, H. A.; Tonta, M. A.; Xiong, Z.; Li, D.; Thomas, S.; Liu, M.; Fallon, J. B.; Parkington, H. C.; Forsythe, J. S. Rapid electrophoretic deposition of biocompatible graphene coatings for high-performance recording neural electrodes. *Nanoscale.* **2022**, *14*, 15845-15858.
129. Xiao, G.; Song, Y.; Zhang, Y.; Xing, Y.; Xu, S.; Lu, Z.; Wang, M.; Cai, X. Cellular-scale microelectrode arrays to monitor movement-related neuron activities in the epileptic hippocampus of awake mice. *IEEE Trans Biomed Eng.* **2021**, *68*, 19-25.
130. Huang, W. C.; Hung, C. H.; Lin, Y. W.; Zheng, Y. C.; Lei, W. L.; Lu, H. E. Electrically copolymerized polydopamine melanin/poly(3,4-ethylenedioxythiophene) applied for bioactive multimodal neural interfaces with induced pluripotent stem cell-derived neurons. *ACS Biomater Sci Eng.* **2022**, *8*, 4807-4818.
131. Saunier, V.; Flahaut, E.; Blatché, M. C.; Bergaud, C.; Maziz, A. Carbon nanofiber-PEDOT composite films as novel microelectrode for neural interfaces and biosensing. *Biosens Bioelectron.* **2020**, *165*, 112413.
132. Yang, X.; Pei, W.; Wei, C.; Yang, X.; Zhang, H.; Wang, Y.; Yuan, M.; Gui, Q.; Liu, Y.; Wang, Y.; Chen, H. Chemical polymerization of conducting polymer poly(3,4-ethylenedioxythiophene) onto neural microelectrodes. *Sens Actuators A Phys.* **2023**, *349*, 114022.
133. Lim, T.; Kim, M.; Akbarian, A.; Kim, J.; Tresco, P. A.; Zhang, H. Conductive polymer enabled biostable liquid metal electrodes for bioelectronic applications. *Adv Healthc Mater.* **2022**, *11*, e2102382.
134. Ganji, M.; Hossain, L.; Tanaka, A.; Thunemann, M.; Halgren, E.; Gilja, V.; Devor, A.; Dayeh, S. A. Monolithic and scalable Au nanorod substrates improve PEDOT-metal adhesion and stability in neural electrodes. *Adv Healthc Mater.* **2018**, *7*, e1800923.
135. Wei, B.; Liu, J.; Ouyang, L.; Kuo, C. C.; Martin, D. C. Significant

enhancement of PEDOT thin film adhesion to inorganic solid substrates with EDOT-acid. *ACS Appl Mater Interfaces.* **2015**, *7*, 15388-15394.
136. Istif, E.; Mantione, D.; Vallan, L.; Hadziioannou, G.; Brochon, C.; Cloutet, E.; Pavlopoulou, E. Thiophene-based aldehyde derivatives for functionalizable and adhesive semiconducting polymers. *ACS Appl Mater Interfaces.* **2020**, *12*, 8695-8703.
137. Tian, F.; Yu, J.; Wang, W.; Zhao, D.; Cao, J.; Zhao, Q.; Wang, F.; Yang, H.; Wu, Z.; Xu, J.; Lu, B. Design of adhesive conducting PEDOT-MeOH:PSS/PDA neural interface via electropolymerization for ultrasmall implantable neural microelectrodes. *J Colloid Interface Sci.* **2023**, *638*, 339-348.
138. Desroches, P. E.; Silva, S. M.; Gietman, S. W.; Quigley, A. F.; Kapsa, R. M. I.; Moulton, S. E.; Greene, G. W. Lubricin (PRG4) antiadhesive coatings mitigate electrochemical impedance instabilities in polypyrrole bionic electrodes exposed to fouling fluids. *ACS Appl Bio Mater.* **2020**, *3*, 8032-8039.
139. Wellens, J.; Deschaume, O.; Putzeys, T.; Eyley, S.; Thielemans, W.; Verhaert, N.; Bartic, C. Sulfobetaine-based ultrathin coatings as effective antifouling layers for implantable neuroprosthetic devices. *Biosens Bioelectron.* **2023**, *226*, 115121.
140. Jeong, J. O.; Kim, S.; Park, J.; Lee, S.; Park, J. S.; Lim, Y. M.; Lee, J. Y. Biomimetic nonbiofouling polypyrrole electrodes grafted with zwitterionic polymer using gamma rays. *J Mater Chem B.* **2020**, *8*, 7225-7232.
141. Lee, Y.; Shin, H.; Lee, D.; Choi, S.; Cho, I. J.; Seo, J. A lubricated nonimmunogenic neural probe for acute insertion trauma minimization and long-term signal recording. *Adv Sci (Weinh).* **2021**, *8*, e2100231.
142. Jain, V.; Forssell, M.; Tansel, D. Z.; Goswami, C.; Fedder, G. K.; Grover, P.; Chamanzar, M. Focused epicranial brain stimulation by spatial sculpting of pulsed electric fields using high density electrode arrays. *Adv Sci (Weinh).* **2023**, *10*, e2207251.
143. Chen, Z.; Liu, X.; Ding, J.; Tian, Y.; Zhang, Y.; Wei, D.; Sun, J.; Luo, F.; Zhou, L.; Fan, H. Tissue-like electrophysiological electrode interface construction by multiple crosslinked polysaccharide-based hydrogel. *Carbohydr Polym.* **2022**, *296*, 119923.
144. Fabbro, A.; Prato, M.; Ballerini, L. Carbon nanotubes in neuroregeneration and repair. *Adv Drug Deliv Rev.* **2013**, *65*, 2034-2044.
145. Ramer, L. M.; Ramer, M. S.; Bradbury, E. J. Restoring function after spinal cord injury: towards clinical translation of experimental strategies. *Lancet Neurol.* **2014**, *13*, 1241-1256.
146. Ye, L.; Ji, H.; Liu, J.; Tu, C. H.; Kappl, M.; Koynov, K.; Vogt, J.; Butt, H. J. Carbon nanotube-hydrogel composites facilitate neuronal differentiation while maintaining homeostasis of network activity. *Adv Mater.* **2021**, *33*, e2102981.
147. Tian, G.; Yang, D.; Chen, C.; Duan, X.; Kim, D. H.; Chen, H. Simultaneous presentation of dexamethasone and nerve growth factor via layered carbon nanotubes and polypyrrole to interface neural cells. *ACS Biomater Sci Eng.* **2023**, *9*, 5015-5027.
148. Wei, W.; Hao, M.; Zhou, K.; Wang, Y.; Lu, Q.; Zhang, H.; Wu, Y.; Zhang, T.; Liu, Y. In situ multimodal transparent electrophysiological hydrogel for in vivo miniature two-photon neuroimaging and electrocorticogram analysis. *Acta Biomater.* **2022**, *152*, 86-99.
149. Lee, J.; Jeong, H.; Kim, J.; Seo, J. M. Investigation of neural electrode fabrication process on Polycarbonate substrate. *Annu Int Conf IEEE Eng Med Biol Soc.* **2022**, *2022*, 3089-3092.
150. Baek, C.; Kim, J.; Lee, Y.; Seo, J. M. Fabrication and evaluation of cyclic olefin copolymer based implantable neural electrode. *IEEE Trans Biomed Eng.* **2020**, *67*, 2542-2551.
151. Altuna, A.; Menendez de la Prida, L.; Bellistri, E.; Gabriel, G.; Guimerá, A.; Berganzo, J.; Villa, R.; Fernández, L. J. SU-8 based microprobes with integrated planar electrodes for enhanced neural depth recording. *Biosens Bioelectron.* **2012**, *37*, 1-5.
152. Ware, T.; Simon, D.; Arreaga-Salas, D. E.; Reeder, J.; Rennaker, R.; Keefer, E. W.; Voit, W. Fabrication of responsive, softening neural interfaces. *Adv Funct Mater.* **2012**, *22*, 3470-3479.
153. Castagnola, E.; Ansaldo, A.; Fadiga, L.; Ricci, D. Chemical vapour deposited carbon nanotube coated microelectrodes for intracortical neural recording. *Phys Status Solidi B.* **2010**, *247*, 2703-2707.
154. Choi, D. S.; Fung, A. O.; Moon, H.; Villareal, G.; Chen, Y.; Ho, D.; Presser, N.; Stupian, G.; Leung, M. Detection of neural signals with vertically grown single platinum nanowire-nanobud. *J Nanosci Nanotechnol.* **2009**, *9*, 6483-6486.
155. Paik, S. J.; Cho, D. D. Development of recording microelectrodes with low surface impedance for neural chip applications. *J Korean Phys Soc.* **2002**, *41*, 1046-1049.
156. Niederhoffer, T.; Vanhoestenberghe, A.; Lancashire, H. T. Methods of poly(3,4)-ethylenedioxithiophene (PEDOT) electrodeposition on metal electrodes for neural stimulation and recording. *J Neural Eng.* **2023**, *20*, 011002.
157. Wang, Y.; Graham, E. S.; Unsworth, C. P. Superior galvanostatic electrochemical deposition of platinum nanograss provides high performance planar microelectrodes forin vitroneural recording. *J Neural Eng.* **2021**, *18*, 0460d0468.
158. Zhang, C.; Driver, N.; Tian, Q.; Jiang, W.; Liu, H. Electrochemical deposition of conductive polymers onto magnesium microwires for neural electrode applications. *J Biomed Mater Res A.* 2**018**, *106*, 1887-1895.
159. Abidian, M. R.; Martin, D. C. Multifunctional nanobiomaterials for neural interfaces. *Adv Funct Mater.* **2009**, *19*, 573-585.
160. Heo, D. N.; Kim, H. J.; Lee, Y. J.; Heo, M.; Lee, S. J.; Lee, D.; Do, S. H.; Lee, S. H.; Kwon, I. K. Flexible and highly biocompatible nanofiber-based electrodes for neural surface interfacing. *ACS Nano.* **2017**, *11*, 2961-2971.
161. Jenkins, P. M.; Laughter, M. R.; Lee, D. J.; Lee, Y. M.; Freed, C. R.; Park, D. A nerve guidance conduit with topographical and biochemical cues: potential application using human neural stem cells. *Nanoscale Res Lett.* **2015**, *10*, 972.
162. James, C. D.; Davis, R.; Meyer, M.; Turner, A.; Turner, S.; Withers, G.; Kam, L.; Banker, G.; Craighead, H.; Isaacson, M.; Turner, J.; Shain, W. Aligned microcontact printing of micrometer-scale poly-L-lysine structures for controlled growth of cultured neurons on planar microelectrode arrays. *IEEE Trans Biomed Eng.* **2000**, *47*, 17-21.
163. Beom Jun, S.; Hynd, M.; Dowell-Mesfin, N.; Smith, K.; Turner, J.; Shain, W.; June Kim, S. Synaptic connectivity of a low density patterned neuronal network produced on the poly-L-lysine stamped microelectrode array. *Conf Proc IEEE Eng Med Biol Soc.* **2005**, *2005*, 7604-7607.
164. Mehenti, N. Z.; Tsien, G. S.; Leng, T.; Fishman, H. A.; Bent, S. F. A model retinal interface based on directed neuronal growth for single cell stimulation. *Biomed Microdevices.* **2006**, *8*, 141-150.
165. Seo, K. J.; Hill, M.; Ryu, J.; Chiang, C. H.; Rachinskiy, I.; Qiang, Y.; Jang, D.; Trumpis, M.; Wang, C.; Viventi, J.; Fang, H. A soft, high-density neuroelectronic array. *Npj Flex Electron.* **2023**, *7*, 40.
166. Roh, H.; Yoon, Y. J.; Park, J. S.; Kang, D. H.; Kwak, S. M.; Lee, B. C.;

Im, M. Fabrication of high-density out-of-plane microneedle arrays with various heights and diverse cross-sectional shapes. *Nanomicro Lett.* **2021**, *14*, 24.
167. Ando, D.; Teshima, T. F.; Zurita, F.; Peng, H.; Ogura, K.; Kondo, K.; Weiß, L.; Hirano-Iwata, A.; Becherer, M.; Alexander, J.; Wolfrum, B. Filtration-processed biomass nanofiber electrodes for flexible bioelectronics. *J Nanobiotechnology.* **2022**, *20*, 491.
168. Mailley, S. C.; Hyland, M.; Mailley, P.; McLaughlin, J. M.; McAdams, E. T. Electrochemical and structural characterizations of electrodeposited iridium oxide thin-film electrodes applied to neurostimulating electrical signal. *Mater Sci Eng C.* **2002**, *21*, 167-175.
169. Stöver, T.; Paasche, G.; Lenarz, T.; Ripken, T.; Breitenfeld, P.; Lubatschowski, H.; Fabian, T. Development of a drug delivery device: using the femtosecond laser to modify cochlear implant electrodes. *Cochlear Implants Int.* **2007**, *8*, 38-52.
170. Henle, C.; Raab, M.; Cordeiro, J. G.; Doostkam, S.; Schulze-Bonhage, A.; Stieglitz, T.; Rickert, J. First long term in vivo study on subdurally implanted micro-ECoG electrodes, manufactured with a novel laser technology. *Biomed Microdevices.* **2011**, *13*, 59-68.
171. Li, L.; Jiang, C.; Li, L. Hierarchical platinum–iridium neural electrodes structured by femtosecond laser for superwicking interface and superior charge storage capacity. *Bio-des Manuf.* **2022**, *5*, 163-173.
172. Yang, Q.; Hu, Z.; Seo, M. H.; Xu, Y.; Yan, Y.; Hsu, Y. H.; Berkovich, J.; Lee, K.; Liu, T. L.; McDonald, S.; Nie, H.; Oh, H.; Wu, M.; Kim, J. T.; Miller, S. A.; Jia, Y.; Butun, S.; Bai, W.; Guo, H.; Choi, J.; Banks, A.; Ray, W. Z.; Kozorovitskiy, Y.; Becker, M. L.; Pet, M. A.; MacEwan, M. R.; Chang, J. K.; Wang, H.; Huang, Y.; Rogers, J. A. High-speed, scanned laser structuring of multi-layered eco/bioresorbable materials for advanced electronic systems. *Nat Commun.* **2022**, *13*, 6518.
173. Amini, S.; Seche, W.; May, N.; Choi, H.; Tavousi, P.; Shahbazmohamadi, S. Femtosecond laser hierarchical surface restructuring for next generation neural interfacing electrodes and microelectrode arrays. *Sci Rep.* **2022**, *12*, 13966.
174. Won, D.; Kim, J.; Choi, J.; Kim, H.; Han, S.; Ha, I.; Bang, J.; Kim, K. K.; Lee, Y.; Kim, T. S.; Park, J. H.; Kim, C. Y.; Ko, S. H. Digital selective transformation and patterning of highly conductive hydrogel bioelectronics by laser-induced phase separation. *Sci Adv.* **2022**, *8*, eabo3209.
175. Pant, M.; Singh, R.; Negi, P.; Tiwari, K.; Singh, Y. A comprehensive review on carbon nano-tube synthesis using chemical vapor deposition. *Mater Today Proc.* **2021**, *46*, 11250-11253.
176. Ansaldo, A.; Castagnola, E.; Maggiolini, E.; Fadiga, L.; Ricci, D. Superior electrochemical performance of carbon nanotubes directly grown on sharp microelectrodes. *ACS Nano.* **2011**, *5*, 2206-2214.
177. Lee, M.; Lee, S.; Kim, J.; Lim, J.; Lee, J.; Masri, S.; Bao, S.; Yang, S.; Ahn, J. H.; Yang, S. Graphene-electrode array for brain map remodeling of the cortical surface. *NPG Asia Mater.* **2021**, *13*, 65.
178. Bakhshaee Babaroud, N.; Palmar, M.; Velea, A. I.; Coletti, C.; Weingärtner, S.; Vos, F.; Serdijn, W. A.; Vollebregt, S.; Giagka, V. Multilayer CVD graphene electrodes using a transfer-free process for the next generation of optically transparent and MRI-compatible neural interfaces. *Microsyst Nanoeng.* **2022**, *8*, 107.
179. Lee, J. Y.; Bashur, C. A.; Goldstein, A. S.; Schmidt, C. E. Polypyrrole-coated electrospun PLGA nanofibers for neural tissue applications. *Biomaterials.* **2009**, *30*, 4325-4335.
180. Mousavi, H.; Ferrari, L. M.; Whiteley, A.; Ismailova, E. Kinetics and physicochemical characteristics of electrodeposited PEDOT:PSS thin film growth. *Adv Electron Mater.* **2023**, *9*, 2201282.
181. Yang, M.; Yang, T.; Deng, H.; Wang, J.; Ning, S.; Li, X.; Ren, X.; Su, Y.; Zang, J.; Li, X.; Luo, Z. Poly(5-nitroindole) thin film as conductive and adhesive interfacial layer for robust neural interface. *Adv Funct Mater.* **2021**, *31*, 2105857.
182. Skoog, S. A.; Kumar, G.; Narayan, R. J.; Goering, P. L. Biological responses to immobilized microscale and nanoscale surface topographies. *Pharmacol Ther.* **2018**, *182*, 33-55.
183. Newman, P.; Galenano Niño, J. L.; Graney, P.; Razal, J. M.; Minett, A. I.; Ribas, J.; Ovalle-Robles, R.; Biro, M.; Zreiqat, H. Relationship between nanotopographical alignment and stem cell fate with live imaging and shape analysis. *Sci Rep.* **2016**, *6*, 37909.
184. Zijl, S.; Vasilevich, A. S.; Viswanathan, P.; Helling, A. L.; Beijer, N. R. M.; Walko, G.; Chiappini, C.; de Boer, J.; Watt, F. M. Micro-scaled topographies direct differentiation of human epidermal stem cells. *Acta Biomater.* **2019**, *84*, 133-145.
185. Simitzi, C.; Ranella, A.; Stratakis, E. Controlling the morphology and outgrowth of nerve and neuroglial cells: The effect of surface topography. *Acta Biomater.* **2017**, *51*, 21-52.
186. Luo, J.; Walker, M.; Xiao, Y.; Donnelly, H.; Dalby, M. J.; Salmeron-Sanchez, M. The influence of nanotopography on cell behaviour through interactions with the extracellular matrix - a review. *Bioact Mater.* **2022**, *15*, 145-159.
187. Geiger, B.; Spatz, J. P.; Bershadsky, A. D. Environmental sensing through focal adhesions. *Nat Rev Mol Cell Biol.* **2009**, *10*, 21-33.
188. Lord, M. S.; Foss, M.; Besenbacher, F. Influence of nanoscale surface topography on protein adsorption and cellular response. *Nano Today.* **2010**, *5*, 66-78.
189. Kim, M. H.; Park, M.; Kang, K.; Choi, I. S. Neurons on nanometric topographies: insights into neuronal behaviors in vitro. *Biomater Sci.* **2014**, *2*, 148-155.
190. Arora, S.; Lin, S.; Cheung, C.; Yim, E. K. F.; Toh, Y. C. Topography elicits distinct phenotypes and functions in human primary and stem cell derived endothelial cells. *Biomaterials.* **2020**, *234*, 119747.
191. Curtis, A.; Wilkinson, C. Topographical control of cells. *Biomaterials.* **1997**, *18*, 1573-1583.
192. Nowduri, B.; Schulte, S.; Decker, D.; Schäfer, K. H.; Saumer, M. Biomimetic nanostructures fabricated by nanoimprint lithography for improved cell-coupling. *Adv Funct Mater.* **2020**, *30*, 2004227.
193. Tringides, C. M.; Boulingre, M.; Khalil, A.; Lungjangwa, T.; Jaenisch, R.; Mooney, D. J. Tunable conductive hydrogel scaffolds for neural cell differentiation. *Adv Healthc Mater.* **2023**, *12*, e2202221.
194. Wang, J.; Wang, H.; Mo, X.; Wang, H. Reduced graphene oxide-encapsulated microfiber patterns enable controllable formation of neuronal-like networks. *Adv Mater.* **2020**, *32*, e2004555.

Received: September 30, 2023
Revised: November 13, 2023
Accepted: November 24, 2023
Available online: December 28, 2023